Development and functional characterization of composite freeze dried wafers for potential delivery of low dose aspirin for elderly people with dysphagia

Smirna Farias[1], Joshua S. Boateng[*1]

Department of Pharmaceutical, Chemical and Environmental Sciences, Faculty of Engineering and Science, University of Greenwich at Medway, Chatham Maritime, Kent, UK, ME4 4TB

**Correspondence: j.s.boateng@gre.ac.uk, joshboat40@gmail.com (Dr Joshua Boateng)*

Abstract

The impact of demographic ageing is likely to be of major significance in the coming decades due to low birth rates and higher life expectancy. Older people generally require more prescribed medicines due to the presence of multiple conditions such as dysphagia which can make swallowing medicines challenging. This study involves the development, characterization and optimization of composite wafers for potential oral and buccal delivery of low dose aspirin to prevent thrombosis in elderly patients with dysphagia. Blank (BLK) wafers (no loaded drug) were initially formulated by dissolving combinations of metolose (MET) with carrageenan (CAR) and MET with low molecular weight chitosan (CS) in different weight ratios in water, to identify optimum polymer combinations. However, drug loaded (DL) wafers were prepared using 45% v/v ethanol to help complete solubilization of the aspirin. The formulations were characterized using texture analyzer (hardness, mucoadhesion), scanning electron microscopy (SEM), X-ray diffractometry (XRD), attenuated total reflection – Fourier transform infrared (ATR-FTIR), differential scanning calorimetry (DSC), thermogravimetric analyzer (TGA), and swelling capacity. Wafers with higher total polymer concentration were more resistant to penetration (MET:CAR 1:1 samples B2, C2) and MET:CS 1:1 (sample E2) and MET:CS 3:1 (sample F2) and also depended on the ratios between the polymers used. From the characterization, samples C2, B2, E2 and F2 showed the most ideal characteristics. XRD showed that BLK wafers were amorphous, whilst the DL wafers were crystalline due to the presence of aspirin. SEM confirmed the presence of pores within the polymer matrix of the BLK wafers, whilst DL wafers showed a more compact polymeric matrix with aspirin dispersed over the surface. The DL wafers showed a good flexibility required for transportation and patient handling and showed higher swelling capacity and adhesion values with phosphate buffer saline (PBS) than with simulated saliva (SS). Drug dissolution studies showed that aspirin was rapidly released in the first 20 minutes and then continuously over 1 hour. FTIR confirmed the interaction of aspirin with the polymers evidenced by peak shifts around 1750 cm^{-1} and the broad peak between 2500 to3300 cm^{-1}. Lyophilized CAR: CS 1:3 (sample DL13), MET:CS 1:3 (sample DL8) and MET:CAR 3:1 (sample DL1) wafers seem to be a very promising system for the administration of low dose aspirin for older patients with dysphagia.

Key words: Aspirin, low molecular weight chitosan, dysphagia, carrageenan, geriatric patients, metolose, wafers

1. Introduction

Over the past few decades, there has been an increased interest in novel drug delivery systems, to improve safety, efficacy and patient compliance and increase the product patent life cycle (Panda, et al., 2012). Fast dissolving and sustained release lyophilized wafers and films are examples of novel formulations for oral and buccal mucosa drug delivery and can be used as fast dissolving oral strips (Peh & Wong , 1999).

One of the main uses of aspirin is as an anticoagulant to reduce the clotting action of platelets. This is possible because aspirin exhibits anti-thrombin effect, and administered to prevent the platelets from aggregating to form blood clots, thus reducing the rate of a heart attacks and strokes. When aspirin is used this way, it is referred to as 'low-dose' aspirin and normally given at 75mg per dose (single tablet daily). Low dose aspirin is recommended for people with heart or blood vessel disease and patients who have had heart bypass surgery (British Medical Association , 2014). Most people who suffer from these problems are older (geriatric) patients, who usually also present with other chronic conditions such as dysphagia (difficulty with swallowing). Dysphagia is an increasing problem among the aging population who are a growing demographic, especially in developed countries. Therefore alternative solutions specifically tailored to the special needs of older populations are required by enhancing the development of novel delivery systems that are easy to administer (Theodorakis & Guodmundsson , 2012).

According to Parkash and colleagues various pharmaceutical preparations used for geriatric patients are being examined to enhance the treatment compliance and improve the quality of life for these patients (Parkash, et al., 2011). To mitigate this problem of dysphagia, fast disintegrating dosage forms such as oral disintegrating tablets, are expected to disintegrate or dissolve in the oral cavity without drinking water, where they disintegrate to release the drug and easily drift down along the esophagus with the help of saliva (Kianfar, et

al., 2011). Using fast disintegrating dosage forms allow rapid therapeutic intervention because of increased bioavailability arising from the rapid release and rapid absorption through the oral mucosa, pharynx, and esophagus and eventually through the gastrointestinal tract. The risk of suffocating during conventional oral administration is also avoided when using fast disintegrating dosage forms, thus improving patient safety (Parkash, et al., 2011).

Likewise, oral mucosa delivery approaches, such as sublingual delivery (under the tongue), buccal delivery, (through the mucosal membranes lining the cheeks) and local delivery, (Shojaei, 1998), offer advantages for improved drug administration including prolonged residence time, ease of application and controlled drug release (Ayensu, et al., 2012). These type of dosage forms are convenient not only for elderly patients, but also the disabled, travelers and busy people who do not always have access to water. There has been an increased interest in use of the oral mucosa for drug delivery because of its ability to avoid first pass metabolism in the liver as well as avoiding gastric acid and enzyme degradation in the stomach and small intestines respectively, which are commonly encountered with the traditional gastrointestinal oral route (Sattar, et al., 2014).

Wafers can possess adhesive properties when formulated with mucoadhesive polymers such as low molecular weight chitosan (CS), metolose (MET), carrageenan (CAR). CS exhibits viscous appearance when hydrated, possesses bioadhesive properties and is biodegradable and biocompatible with low toxicity (Siriwat, et al., 2012). Degree of deacetylation (DDA) and molecular weight (MW) of chitosans are important to their physical and biological properties including crystallinity, degradation, tensile strengths and moisture contents (Yuan, et al., 2011). MET is a non-ionic cellulose ether composed of methylcellulose and three types of HPMC which are available in different grades with varying viscosities. The most important properties of MET includes solubility in cold water, development of transparent solutions and viscoelastic properties (Khan, et al., 2016).

Carrageenan (CAR) is produced from red seaweed (Rhodophyceae) and is a polysaccharide formed from sulfate group and galactose molecule with a repeating structure of alternating 1,3 – linked D-galactophyranosyl arid 1,4 – linked D-galactophyranosyl units. The 3-linked units occurs as the 2- and 4- sulfate, or non-sulfate, while the 4-linked units occur as the 2-sulfate, the 2,6 disulfate, the 3,6-anhydride, and the 3,6-anhydride-2-sulfate (Stanley, 2010). They are classified into different grades, kappa (κ) which has a linear polysaccharide structure with one sulfate group per two galactose molecules, assuming a helical network which is strengthened with the presence of potassium ions. Iota (ι), assumes a helical conformation but with two sulfate groups per two galactose molecules which forms a soft gel in the presence of calcium ions. Lambda (λ), has three sulfates per two galactose molecules and does not form a helical structure and does not use ions to achieve a viscous solution because it is a non-gelling polysaccharide. CAR as natural polymer has not been widely used in pharmaceutical applications, although there are a lot of published literature reporting on the use of CAR in the form of wafers and films (Tari, et al., 2009). According to Kianfar and co-workers, buccal wafers were obtained by freeze drying gels combining 2% (w/w) k-CAR911 and 4% (w/w) Pluronic F127 incorporating 4.4% (w/w) PEG 600 as well as 0.8% (w/w) ibuprofen or 1.8% (w/w) paracetamol. The texture analysis for these wafers showed ideal mechanical and mucoadhesion characteristics whilst both drugs remained stable over 6 months and drug dissolution at salivary pH showed gradual release within 2 hours, which demonstrate the potential of CAR and pluronic F127 based wafers for buccal mucosa drug delivery (Kianfar et al, 2011, 2013). κ-carrageenan was selected due to the availability of various sites for hydrogens bonding which improves bioadhesive properties to the formulation, as well as, increase in drug bioavailability (Thommes & Kleinebudde, 2006).

The current paper describes the formulation development, characterization and optimization of composite MET:CAR and MET:CS lyophilized wafers as drug delivery

systems via both the oral route and buccal mucosa membrane for potential administration of low dose aspirin to geriatric patients with dysphagia. The formulations have been functionally characterized using texture analysis, X-ray diffraction (XRD), scanning electron microscopy (SEM), attenuated total reflectance – Fourier transform infrared (ATR-FTIR) spectroscopy, differential scanning calorimetry (DSC) and thermogravimetric analysis (TGA) for hardness, mucoadhesion, surface and internal morphology, crystallinity, chemical interactions and thermal behavior respectively. The characterization results were used to compare the properties of MET:CAR and MET:CS wafers to determine which could be suitable for controlled release via buccal mucosa absorption or as fast disintegration dosage forms for easy swallowing.

2. Materials and methods

2.1 Materials

`Metolose (MET) was obtained as a gift from Shin Etsu (Stevenage, Hertfordshire, UK), polyethylene glycol (PEG 400), gelatin and mucin from bovine submaxillary gland were obtained from Sigma-Aldrich (Gillingham, UK), carrageenan (CAR) low viscosity grade NF 911 (κ), molecular weight less than 100,000 Da, 25% sulfate esters, stable at pH values > 3.8 was obtained as a gift from IMCD Ltd (Sutton, UK), low molecular weight chitosan (CS) with 95% degree of deacetylation and MW of 3000 Da .obtained from Qingdao Yuda Century Economy and Trade CO, Ltd (China), calcium chloride, sodium chloride, sodium phosphate dibasic, magnesium chloride hexahydrate, potassium carbonate hemihydrate and sodium phosphate monobasic monohydrate were obtained from Fischer Scientific (Loughborough, UK).

143 *2.2 Formulation optimization*

144 *2.2.1 Preliminary development of composite BLK wafers*

145 Prior to drug loading, preliminary investigations were undertaken by preparing composite
146 blank (BLK) wafers by freeze-drying their aqueous solutions combining MET with CAR
147 (MET:CAR) and MET with CS (MET:CS) in different weight ratios. This was to identify a
148 suitable number of formulations as composite combinations as part of the development and
149 optimization process. The composite gels were prepared by simply dispersing MET:CAR,
150 MET:CS in deionized water and magnetically stirred till homogeneous solutions were
151 obtained. The concentrations prepared are summarized in table 1 a). 1g of each initial BLK
152 composite polymer solution was poured into each well of a 24 multi-well plate (diameter 15.5
153 mm). The freeze-dried process was conducted by an automated lyophilization cycle on a
154 Virtis Advantage XL 70 freeze-dryer (Biopharma process systems, Winchester, UK). In the
155 freezing steps the samples were cooled from room temperature to 5 °C for 40 minutes, 5 °C
156 to – 10 °C for 40 minutes and -10 °C to -55 °C for 120 minutes. An annealing process was
157 integrated into the freezing cycle to boost pore size distribution by increasing the temperature
158 from – 55 °C to – 35 °C over 2 hours and cooling back to – 55 °C over 3 hours and
159 maintained at -55 °C over 1 hour with a condenser temperature of – 55 °C and pressure of
160 200mTorr was implemented to assure uniformity. A pressure of 50mTorr, with temperature
161 increased from -55 °C to – 20 °C during 8 hours and further increased from – 20 °C to – 15
162 °C during 10 hours was applied during the primary drying stage. The secondary drying
163 happened at the same pressure as primary drying and the temperature was raised from – 15
164 °C to 25 °C over 12 hours 30 minutes. Heat was applied in this step to remove the amount of
165 water molecules remained during primary drying after the free ice sublimed (Nireesha, et al.,
166 2013) (Okeke & Boateng, 2016). BLK formulations were not prepared in ethanol as the

polymers used were water soluble. Ethanol was only used in the DL formulations as part of further development to help the solubility of aspirin which is a hydrophobic drug.

2.2.2 Formulation of drug loaded wafers

The drug loaded (DL) composite wafers were prepared by freeze-drying solutions combining MET with CAR and MET with CS in different weight ratios with each wafer loaded with 75 mg of aspirin. The various DL wafers prepared are summarized in (table 1 b). During the drug loading many problems arose including precipitation of aspirin from the aqueous polymer solutions and poor physical properties of the resulting wafers. Therefore ethanol at different concentrations (v/v) and composite formulations comprising two or three polymers were investigated as part of further optimization to obtain DL wafers with the ideal physical properties.

After the preparation of the optimized composite DL polymeric solutions, (1g) was poured into each well of a 24 multi-well plate (diameter 15.5mm) with 75 mg of aspirin per well. To obtain 75 mg per well, the dose was multiplied by the amount of DL solution to be prepared. In a 100 g solution, 7500 mg of aspirin was needed, so that 1 g of solution theoretically contained 75 mg of aspirin. Prior to freeze-drying, the aspirin loaded polymer solutions were frozen in a -80°C freezer to reduce the length of time aspirin remained in an aqueous liquid environment, owing to its known susceptibility to hydrolysis. The samples were then subjected to the freeze-drying cycle as described for the BLK wafers (section 2.2.1), but without the annealing step.

2.3 Texture analysis

Texture analyzer (HD plus, Stable Micro System, Surrey, UK) fitted with a 5 kg load cell, was used to analyze the mechanical and mucoadhesion properties of the wafers. The

191 software Texture Exponent 32® was used to collect and process the data from the texture
192 analyzer. Three replicates (n = 3) were performed for each sample.
193
194 *2.3.1 Mechanical properties of wafers*
195 The resistance of the wafers to deformation, referred to as 'hardness' was measured
196 with the instrument in compression mode. Each wafer was compressed in 5 different
197 positions (n = 3), using a 2mm cylinder stainless steel probe to a depth of 1mm and speed of
198 1 mm/sec.
199 *2.3.2 Mucoadhesion studies*
200 The wafers were attached to an adhesive probe (35 mm diameter) using double-sided
201 adhesive tape. Gelatin gel [6.67% (w/v)], representing the buccal mucosa surface, was
202 prepared by dissolving the gelatin in 70 °C water. 20 ml of the resulting hot solution were
203 transferred into Petri dishes (86 mm diameter) and left in the fridge overnight to set into a
204 solid gel. Before performing the mucoadhesion, 500 µl of PBS pH 6.8 ± 0.1 or simulated
205 saliva (SS) at pH 6.8 ± 0.1 were spread over the surface of the gelatin to mimic the buccal
206 mucosa more accurately. The [0.01 M PBS (pH 6.8 ± 0.1)] was prepared by dissolving 6.80 g
207 of potassium dihydrogen phosphate in 1L of deionized water and adjusting the pH 6.8 ± 0.1
208 using sodium hydroxide (Boateng & Ayensu, 2014). The SS was prepared by dissolving
209 calcium chloride dehydrate (0.228 g), sodium chloride (1.017 g), sodium phosphate dibasic
210 (0.204 g), magnesium chloride hexahydrate (0.061 g), potassium carbonate hemihydrate
211 (0.603 g), sodium phosphate monobasic monohydrate (0.273 g) and submaxillary mucin
212 (1.000 g) in 1L of deionized water (Marques, et al., 2011). The probe with the wafers
213 attached was lowered to make contact with the model mucosa surface with an applied force
214 of 1.0 N and was detached after 60 seconds of contact. The mucoadhesion strength was
215 determined by the maximum adhesive force (F_{max}) necessary to detach the sample from the

model buccal surface. The work of adhesion was determined by the area under the force-distance curve and cohesiveness by the distance the wafers travelled before detaching from the gelatin surface.

2.4 Swelling capacity

The swelling capacity of the BLK and DL wafers was determined in two different media [(0.01M PBS solution (pH 6.8 ± 0.1) and (SS) (pH 6.8 ± 0.1)] and both set at a temperature of 37 ± 0.1°C. The wafers were immersed into 5 ml of the PBS or SS and the percentage swelling capacity was determined by recording the change in weight at specific time intervals up to 120 minutes. For every time point, the media was removed to obtain an accurate weight of the sample and replaced with fresh media. The swelling capacity were determined for three replicates (n = 3) and calculated using equation 1 (Okeke & Boateng, 2016).

Swelling index = $\frac{Ws-Wd}{Wd}$ x 100 (Equation 1)

where; W_d = dry weight of wafers; W_s = weight of wafers after swelling

2.5 Scanning electron microscopy (SEM)

The surface morphology of the BLK and DL wafers were analyzed using a Hitachi SU8030 (Hitachi High-Technologies, Krefeld, Germany). The wafers were cut into small pieces and placed on Agar Scientific G301 aluminium pin-type stubs, using Agar Scientific G3347N double-sided adhesive carbon tape. The wafers were gold coated for clearer pore image using a Sputter Coater (Edwards 188 Sputter Coater S1508) and analyzed at 5.0 kV accelerating voltage.

240 *2.6 Pore analysis*

241 Pore analysis by a solvent displacement method was used to determine the porosity of
242 the composite wafer structure. The wafers were initially weighed and then immersed in 10 ml
243 of ethanol in a 20 ml measuring cup, covered and left to stand for 2 hours for complete
244 saturation. Then, the set up was degassed to remove all air bubbles from the wafers, sample
245 removed from the solvent, quickly wiped to remove excess solvent and immediately re-
246 weighed to avoid the loss of ethanol which is volatile. The porosity (%) of wafers were
247 determined for three replicates (n = 3) and calculated using equation 2 (Okeke & Boateng,
248 2016).

249 $$P = \frac{Vp}{Vg} \times 100 = \frac{Wf - Wi}{PeVg} \quad \text{(Equation 2)}$$

250 where; V_p = pore volume

251 V_g = wafers geometrical volume

252 W_f = final weight of wafer

253 W_i = initial weight of wafer

254 ρ_e = ethanol density (0.789 g/cm^3)

255

256 *2.7 X-ray diffraction (XRD)*

257 X-ray diffraction was used to determine the physical form (crystalline/amorphous) of
258 the BLK and DL wafers using a D8 Advantage X-ray diffractometer. Wafers were
259 compressed using two clean glasses, placed on the holder and mounted on the sample cell.
260 For pure compounds, Mylar was used to hold the powders before placing on the sample cell.
261 The samples were analyzed in transmission mode at diffraction angle range of 5° to 50° 2θ,
262 step size 0.04°, and scan speed of 0.4 s/step.

2.8 Attenuated total reflectance Fourier transform infrared spectroscopy (ATR-FTIR) analysis

ATR-FTIR spectra were obtained from a Perkin Elmer Spectrum instrument equipped with a diamond universal ATR unit. The composite BLK and DL wafers were cut into small pieces and placed on the ATR diamond crystal. Force was applied using the pressure clamp to allow suitable contact between the samples and the diamond crystal. The resolution of the samples were recorded at 4 cm^{-1} within the range of 500-4000 cm^{-1}. Background spectra were subtracted in order to obtain a consistent absorbance of each sample. Pure compounds were analyzed by placing a small amount of the polymer on the ATR diamond crystal followed by the same process used for analyzing wafers.

2.9 Thermogravimetric analysis (TGA)

TGA studies were performed using a Q5000 (TA Instruments, New Castle, DE, US) thermogravimetric analyzer to determine the residual moisture content (%), dynamic weight loss and degradation temperature of the pure polymers, BLK and DL wafers. About 1 to 2 mg of the wafers and the pure compounds was placed into hermetically sealed Tzero aluminium pans. The samples were heated under nitrogen gas at a flow rate of 25 mL/min, from 20 to 300 °C at a heating rate of 10 °C/min.

2.10 Differential scanning calorimetry (DSC)

A DSC Mettler Toledo instrument was used to thermally evaluate the pure compounds, the BLK and DL wafers. The samples were weighed (between 2 and 5 mg), placed in Tzero pans and covered with Tzero hermetic lids and heated from – 25 °C to 250 °C at the rate of 10 °C/min under continuous stream of nitrogen.

288

289 *2.11 In vitro drug release*

290 *In vitro* drug dissolution of aspirin loaded (DL) wafers was performed using a Franz-
291 diffusion cell apparatus. The receptor compartment was filled with 8 ml of two different
292 media [(0.01M PBS solution (pH 6.8 ± 0.1) and SS (pH 6.8 ± 0.1)] with a mesh (1 mm mesh
293 size) on the receptor surface. The donor and receptor compartments were sealed with paraffin
294 to limit evaporation and held together by a pinch clamp. The system was placed on a water
295 bath at 37 °C and magnetically stirred (200 rpm). Formulations were cut, accurately weighed
296 (20-40 mg) and placed on the mesh between the donor and receptor compartments such that
297 the dissolution medium just wet once side of the wafer sample. At predetermined time
298 intervals, 0.5 ml aliquots of the dissolution media were withdrawn using a 1 ml syringe,
299 filtered through a 0.45 μm cellulose acetate membrane, transferred into HPLC vials and
300 analyzed using HPLC. The aliquot withdrawn was always replaced with fresh dissolution
301 medium at 37 °C. The percentage cumulative drug released from the wafers were calculated
302 and plotted against time (n = 3). The dissolution data were fitted to the Korsmeyer-Peppas
303 equation to determine mechanisms of drug release (Khan et al, 2015) (see supplementary data
304 S1).

305

306 *2.12 Statistical analysis*

307 Statistical analysis was carried out to compare swelling capacity %, mucoadhesion, hardness,
308 porosity and drug release of wafers using two tailed student t-test with 95% confidence
309 interval (p-value < 0.05) as the minimum level of significance. All the experiments were
310 carried out in triplicates for all experiments with mean and standard deviation.

3. Results and discussion

3.1 Optimization of formulations

The BLK and the DL formulations were optimized separately because preliminary studies were carried out in order to analyze the physical and chemical properties of the composite polymer formulations. The objective of the preliminary study was to develop an elegant and physically stable formulation showing compatibility between the combined polymers prior to drug loading (Shimoyamada, et al., 1994). The ratios of polymers were optimized in order to obtain a composite formulation with enhanced characteristics compared to that achieved by the individual polymers. The composite formulations were preferred as they possessed enhanced characteristics from both polymer, such as mucoadhesion and mechanical strength In this study the ratios for MET:CAR, CAR:CS and MET:CS were chosen from 1:3, 1:1 and 3:1 to determine the best combinations with ideal characteristics for loading the drug.

The BLK wafers prepared from MET:CAR 1:1 (sample B2), MET:CAR 3:1 (sample C2) and MET:CS 1:1 (sample E2) and MET:CS 3:1 (sample F2) gels were easily removed from the well plates, easy to handle and remained intact when removed from the mold. However, the wafers prepared from MET:CAR (samples A1 and A2) and MET:CS (samples D1 and D2) in the ratio 1:3 were weaker, brittle and easily deformed when handled. Therefore, samples A1, A2, D1 and D2 were tested by texture analyzer to confirm mechanical properties. Wafers prepared from MET:CAR and MET:CS (samples A, B, C, D, E and F) gels at any combination ratio showed the same weak characteristics of the wafers described above, but they were also tested for mechanical characteristics for confirmation of their weakness.

Though the BLK formulations prepared from gels composed of MET:CS ratio 3:1 and 1:1 (sample F2 and E2) showed ideal characteristics and initially attempted for drug loading,

this was challenging due to precipitation of the drug from the aqueous gels. This is due to the fact that only 3 mg/ml of aspirin dissolves in water which was far below what was required to ensure the formulation of low dose aspirin wafers containing 75 mg of the drug similar to the low dose aspirin tablets currently available in the market. Various combinations of ethanol/water were prepared to determine the minimum volume of ethanol required to completely dissolve the aspirin and 45% v/v ethanol was the minimum necessary for the aspirin to completely dissolve in the gels. However, the addition of ethanol affected the freezing procedure originally optimized for preparing the BLK wafers. This is because though organic solvents, are removed during the primary drying step, lower temperatures are required to freeze and condense solvents, compared to water. To resolve this challenge, the annealing step for the freeze-drying cycle used in preparing the BLK formulations was removed during formulation of the DL wafers, with the lowest freezing temperature maintained at -55 °C for 6 hours instead (Barley, 2009).

Further, the use of ethanol also affected the physical behavior of the DL wafers obtained by loading aspirin into the originally optimized BLK gels. As a result, further formulation development of MET:CS and MET:CAR gels containing higher total polymer, in different ratios, were formulated to further optimize the DL wafers. Therefore, wafers prepared from MET:CAR gels in the ratio 3:1 and 1:1 (samples DL1 and DL2) and those prepared from CAR:CS 1:1 and 1:3 (samples DL14 and DL13) and MET:CS 1:3 (sample DL8) were tested with texture analyzer to confirm their ideal mechanical characteristics.

3.2 Texture analysis (TA)

3.2.1 Mechanical properties of the wafers

The resistance to deformation of wafers is an important functional characteristic, as it affects the performance of the wafers in terms of ease of handling and application without

damaging the formulation, which is important to guarantee consistent dosing between administrations (Boateng et al., 2010, Kianfar et al., 2014). Figure 1a shows the hardness (resistance to compressive deformation) profiles of wafers prepared from MET:CS at different polymer ratios and different total polymer content within the original gels. The wafers prepared from MET:CS gels in the ratios 1:3, 1:1 and 3:1 (samples D, E, and F) showed a very low hardness profile compared to those containing higher total polymer content due to lower matrix density of the former. MET:CS ratio 1:3 (sample D2) showed a hardness of 0.42 ± 0.02 N while ratio 3:1 (sample F2) showed a hardness of 0.35 ± 0.15 N and 1.5% (w/v) MET:CS ratio 1:1 (sample E) had a hardness of 0.77 ± 0.16 N. Further, MET:CS ratios 1:3, 1:1 and 3:1 (samples D1, E1 and F1) which had a total solids content of 2% per 100g of gel, showed similar trends to MET:CS wafers containing total solids content of 2% per 100g of gel with hardness values of 1.20 ± 0.08 N, 1.23 ± 0.52 N and 0.88 ± 0.19 N, respectively. The hardness of MET:CS ratio 1:3 (sample D2) showed a value of 1.88 ± 0.76 N, ratio 1:1 (sample E2) was 2.69 ± 0.28 N and ratio 3:1 (sample F2) was 2.86 ± 0.28 N.

The results generally demonstrated that as the concentration of MET increased within the formulation, the hardness of the wafers also increased though they remained non-brittle. The reason was that as the polymer content increased, the resulting gels became more viscous and produced more stable, stronger, compact (denser) wafers after freeze-drying. However, the wafers with higher ratios of CS were very brittle and flaky and difficult to remove for testing. These observations suggest that MET:CS 1:1 and 3:1 (samples E2 and F2) were ideal formulations for loading aspirin, compared to the wafers prepared from gels containing lower total polymer content such as samples D, E and F which deformed easily during removal and handling. Sample D2 had a lower hardness profile compared to sample E2 and F2due to the lower amounts of MET as previously noted.

Figure 1 b shows the hardness profiles of composite MET:CAR wafers in the ratio 1:3, 1:1 and 3:1 (samples A, B, C, A1, B1, C1, A2, B2 and C2). As was the case for MET:CS wafers, the hardness profiles were higher as the ratio of MET increased within the formulation. The wafers prepared from MET:CAR 1:3 (sample A) had a hardness of 0.24 ± 0.06 N, whereas ratio MET:CAR 3:1 (samples C) had a value of 1.25 ± 0.12 N. The hardness of sample A1 was 0.25 ± 0.02 N, and sample B1 was 0.37 ± 0.02 and sample C1 was 2.60 ± 0.04 N. Although, samples C and C1 had higher hardness values, these were lower compared to samples C2 which showed a hardness of 3.57 ± 0.09, which should be an ideal candidate for controlled release of drug.

Comparing MET:CS and MET:CAR wafers, it was demonstrated that MET:CAR formulations were stronger and more resistant to compressive deformation than MET:CS wafers due to the functional and physical properties of CAR which possess stabilizing, gelling and thickening ability (Pairatwachapun, et al., 2016). Due to the high robustness, good compatibility and persistent viscoelasticity, CAR has also been used in tablets as excipient for sustained release formulations (Zia, et al., 2017) due to its ability produce stronger formulations. On the other hand, MET:CS formulations were weaker and brittle due to highly water soluble nature of soluble CS and therefore unable to swell to form stable gels.

Figure 1 c shows the hardness profiles of DL MET:CAR 3:1 (sample DL1) CAR:CS 1:3 (sample DL13) and CS:CS 1:1 (sample DL14) wafers and MET:CS ratios 1:3 and 1:1 (samples DL8 and DL7) wafers . The DL wafer obtained from MET:CAR 3:1 gels (sample DL1) showed the highest hardness value of 5.19 ± 0.03 N and the sample DL2 prepared from MET:CAR 1:1 showed a lower hardness value of 1.58 ± 0.14 N. This shows that increasing MET content when in combination with CAR results in a higher resistance to deformation under compression.

409 Comparing the DL formulations with the BLK, there was an increase in hardness for
410 sample DL2 and sample DL1. This increase can be attributed to the decreased porosity of the
411 wafers due to the added drug and subsequent salt formation including salicylates.
412 Generally, the hardness of the wafers affects the swelling profile of the wafers
413 (Campo, et al., 2009) because wafers with a higher hardness profiles means that the porous
414 matrix is more compacted (see SEM results) and less able to swell which impacts on the rate
415 of drug diffusion.
416
417 *3.2.2 In vitro mucoadhesion*
418 One of the objectives of the current study, was to explore use of freeze-dried wafers to
419 deliver low dose aspirin for patients with dysphagia as an alternative to currently used oral
420 tablets, either as rapid disintegration matrix that is easily swallowed (gastric absorption) or
421 formulations that can remain long enough in the buccal region to allow pregastric absorption,
422 followed by swallowing of the remaining free flowing gel. Therefore, it was important to
423 determine the mucoadhesion behavior of the formulated wafers. There are different theories
424 to explain the mucoadhesion process (Smart, 2005). Mucoadhesive bond formation involves
425 wetting and swelling of the polymer network arising from intimate contact between the
426 substrate and dissolution fluid such as PBS or SS followed by interpenetration and
427 entanglement between polymer chains and the mucosal substrate (Sriamornsak, et al., 2008).
428 Figure 2a – b shows the mucoadhesion profiles of BLK MET:CAR and MET:CS wafers
429 obtained from the texture analyzer. Figure 2 a showed that the peak adhesion force (PAF) in
430 PBS for MET:CAR formulations was higher when the ratio was 1:1 with value of 0.54 ± 0.05
431 N for sample B1 and 0.54 ± 0.01 N for sample B2. The PAF for the wafers composed of
432 MET:CAR ratio 3:1 (samples C1 and C2) also showed higher values at 0.52 ± 0.13 N and
433 0.41 ± 0.01 N, respectively, compared with MET:CAR 1:3 (samples A1 and A2). . Samples

A1 showed higher TWA values of 1.11 ± 0.20 N mm and 0.53 ± 0.32 N mm for sample A2 compared to samples B1, C1, B2 and C2 with TWA values of 0.43 ± 0.01, 0.44 ± 0.01 N mm and 0.19 ± 0.07, 0.21 ± 0.01 N mm respectively. The increase in the TWA for samples A1 and A2 wafers is attributed to the higher concentration of CAR in the formulations which impart bioadhesive properties by the availability of several sites for hydrogen bonding. In addition, CAR enhances the mucoadhesive properties by the negative charge of the sulfate group in its structure forming ionic bonds with the positively charged mucin present on the model buccal mucosa membrane (Kianfar, et al., 2011).

The cohesiveness values were also affected by the different ratios and total polymer content. Sample A1 showed the highest cohesiveness of 4.84 ± 0.61 mm which was decreased to 0.63 ± 0.02 mm for sample C1. For sample A2, the cohesiveness was 2.46 ± 0.38 mm but decreased to 0.87 ± 0.03 for sample C2 due the CAR characteristics explained above. The cohesiveness in the SS decreased when compared with PBS, and there was a slight difference between the cohesiveness for sample A1 with values within 1.31 ± 0.38 mm increasing slightly to 1.38 ± 0.09 mm for sample C1 in SS. For sample A2 there was a decrease from 2.46 ± 0.38 mm to 0.87 ± 0.03 mm for sample C2. The TWA for SS increased from 0.15 ± 0.03 N mm for sample A1 to 0.45 ± 0.12 N mm in sample C1.. Similar values were obtained for samples A2 and C2. .

Figure 2b shows the mucoadhesive profiles of MET:CS wafers obtained from gels containing total polymer solids of 2.0 and 2.5% in the gels. The PAF and TWA increased with increased amounts of MET with a maximum PAF value of 0.41 ± 0.01 N for sample F1 and 0.48 ± 0.06 N for sample F2 in both PBS and SS. The TWA increased from 0.16 ± 0.01 N mm in sample D1 to 0.29 ± 0.05 N mm in sample F2. However, the cohesiveness for samples D1, E1, F1, D2, E2 and F2 in PBS were very similar to SS and was not affected by the total polymer content or weight ratios. This could be because cohesiveness represents the

459 distance travelled by the wafer before being detached from the model mucosa surface, and
460 mainly a function of the actual polymer contents rather than how much was present. The
461 latter impacts on the initial rate of hydration which affects PAF and TWA more than
462 cohesiveness (Boateng and Ayensu, 2014).

463 Figure 3a - b shows the mucoadhesion profiles of DL composite wafers prepared
464 from MET:CAR 1:1 (sample DL2) and 3:1 (sample DL3), CAR:CS 1:3 (sample DL13) and
465 1:1 (sample DL14) and MET:CS ratio 1:3 (sample DL8) in the two different media. The
466 results showed a similar behavior to the corresponding BLK wafers (figure 2 a) with a
467 decrease in PAF, cohesiveness and TWA for the formulations containing lower amounts of
468 MET in the case of MET:CAR wafers and a decrease in PAF and TWA for MET:CS
469 formulations as the CS ratio increased. However, in the case of CAR:CS formulations, there
470 was an increase in cohesiveness from 0.73 ± 0.11 mm to 1.14 ± 0.11 mm as the ratio of CS
471 increased which can be attributed to the fact that increasing amount of CS in CAR:CS
472 formulations allows easier formation of a gel like structure upon hydration and helps more
473 intimate contact with the substrate. According to Tobyn et al. (1997), increasing ionic
474 strength of the media and the presence of sodium and potassium ions results in decreased
475 adhesion when the amount of CAR is higher in the formulation.
476
477 The effect of ionic strength and pH on swelling and mucoadhesion of polymer
478 matrices has been described by (Park & Robinson, 1985). They found out that the strength of
479 mucoadhesion attraction at the mucosal membrane for polymers possessing carboxyl groups
480 were much stronger than that those with neutral functional groups such as non-polar
481 polymers. The pH of the saliva as medium affects the behaviors of the polymer depending on
482 the salivary flow rate and method used to determine it. The pH of the surrounding medium to
483 which mucoadhesive polymers come in contact can alter the ionization state and the adhesion

properties of the polymers. This could explain the differences and similarities observed in the mucoadhesion profiles in the two different media (SS and PBS), however, SS is the most realistic media simulating *in vivo* conditions more closely.

3.3 Swelling studies

For hydrophilic polymer based matrices such as the composite wafers formulated in the current study, the swelling is an important characteristic, as it affects other functional properties, including mucoadhesion, rate of disintegration, drug dissolution and eventual release from the swollen or eroded matrix. It depends on several physical properties of the matrix, including porosity, matrix density and mechanical strength. During swelling, polymer chains absorb moisture, and converted from glassy state to the rubbery state, resulting in increased chain mobility, which allows dissolution of dispersed drug and its subsequent diffusion out of the swollen matrix. The swelling also depends on other external factors such as pH, ionic strength and total volume of the dissolution medium, therefore the % swelling capacity (index) of the wafers was also determined in two different media i.e. SS and PBS.

The % swelling index for MET:CS 3:1 wafers (samples C1 and C2) was observed to be 849 ± 62.88% and 803 ± 91.50% in SS (Figure 4a) and higher at 1413 ± 240% and 914 ± 168% in PBS for MET:CS 3:1 wafers i.e. samples C1 and C2 respectively (Figure 4b). Samples C1 and C2 had a higher swelling capacity over a longer period compared to MET:CS 1:1 and 1:3 wafers (samples B1, A1) and MET:CS 1:1 and 1:3 (samples B2 and A2) which is attributed to the higher amount of MET in the formulation. Samples D1 and D2 had very low swelling capacity and disintegrated within seconds after being placed in SS due to the lower amounts of the swellable MET.

However, samples A1 and A2 showed a higher % swelling capacity compared to samples B1, B2, C1 and C2 which is attributed to the higher ratio of MET in the formulations, due to

509 the higher density of MET in the wafers and corresponded with their higher resistance to
510 compression.

511 The % swelling capacity for MET:CAR 1:3 wafers (samples A1 and A2) were 2822 ±
512 60% and 2257 ± 183% respectively within 5 minutes in SS (Figure 4c). These wafers had
513 higher ability to swell in SS compared to the others due to the higher ratio of CAR which
514 increases pore sizes and its distributions thus increasing the rate of water ingress (hydration)
515 and subsequently % swelling capacity. In figure 4 c it can be observed that the MET:CAR 1:1
516 and 3:1 wafers (samples B1, B2, C1 and C2) had longer swelling duration of about 120
517 minutes and lower swelling capacity which is due to the higher concentrations of MET which
518 act as a stabilizer for the wafers (Shin Etsu Chemical, 2005). In SS the swelling profile of
519 MET:CAR 3:1,1:1 and 1:3 (samples A1, B1, C1, A2, B2 and C2) were lower than when
520 performed in PBS (Figure 4d) which could be due to the difference in ionic strength of the
521 media and that plays an important role in the swelling of the wafers (Khan, et al., 2016).
522 These characteristics confirm the MET:CAR wafers as potentially suitable for a controlled
523 release of the low dose aspirin and the MET:CS suitable as a fast disintegrating wafers as
524 observed during the mechanical testing.

525 The swelling capacity (%) in PBS (Figure 5a) for the DL wafers prepared from
526 MET:CAR 3:1 and 1:1 (samples DL1 and DL2) gels showed the highest swelling capacity of
527 313 ± 21 and 540 ± 40 % respectively. They were able to maintain their structural integrity at
528 the beginning of the experiment, but after 30 minutes they lost their integrity because of
529 excessive absorption of water molecules. Between the wafers produced from CAR:CS 1:3
530 and 1:1 (samples DL14 and DL13) a fast disintegration of the DL wafers were observed
531 within 2 minutes with maximum swelling capacity of 154 ± 10 % and 215 ± 23 %
532 respectively. This showed that as the concentration of CAR increased, the swelling capacity
533 increased and this was similar for MET:CAR 1:1 and 3:1 wafer (samples DL1 and DL2).

534 Figure 5b shows the swelling capacity % of the DL wafers in SS. The results shows similar
535 profiles for the wafers produced from MET:CAR 3:1 and 1:1 (samples DL1 and DL2) with a
536 decrease in the swelling capacity as MET concentration increased, at 302 ± 52 % and 527 ±
537 69 respectively. The rate of swelling of MET:CAR wafers in PBS was higher than the rate of
538 swelling in SS media indicating that MET:CAR wafers exhibited faster rate of water uptake
539 and hydration in PBS than in SS.

540 Generally the BLK samples A2 and C2 showed higher % swelling capacity compared
541 to the corresponding DL samples DL1 and DL2 in both media. The reason behind the BLK
542 wafers showing higher swelling capacity (%) compared to DL wafers is due to the formation
543 of sodium sulfate in the latter which affects their swelling capacity (Khan, et al., 2016).
544 Further, the swelling capacity values were lower in SS when compared with PBS which can
545 be attributed to the difference in ionic strength of the media which plays an important role in
546 the swelling profile of porous formulations such as wafers (Peh & Wong, 1999).

547

548 *3.4 Scanning electron microscopy*

549 Figure 6a - d showed a porous sponge-like micro structure for the MET:CAR wafers resulting
550 from the sublimation of water during freeze-drying process. Samples A, B, C, A1, B1, C1,
551 A2, B2 and C2 showed collapsed pore walls as the concentration of MET increased with the
552 most collapsed walls observed in samples C1 and C2. Figure 6e - h show the surface
553 morphology of BLK MET:CS wafers which also demonstrated a sponge-like and porous
554 structure, and showed highly collapsed pore walls irrespective of the different polymer ratios
555 which is attributed to the presence of a low molecular weight compound (soluble CS) which
556 has high affinity for water therefore affecting ice crystal formation and crystal size during the
557 freeze drying process, and therefore pore size which subsequently affects rate of hydration,
558 swelling, mucoadhesion and drug release.

559 Although, the BLK MET:CAR wafers showed smaller pores that were more
560 uniformly distributed compared to MET:CS wafers, the BLK MET:CS wafers were more
561 brittle in appearance compared with BLK MET:CAR which can be attributed to the presence
562 of sub pores. This explains the reason of MET:CAR formulations being more resistant to
563 deformation (hardness) than MET:CS wafers.
564 Figure 7a shows the surface features of the aspirin crystals at x30 magnification. It
565 was observed that the aspirin crystal is smooth and that small crystallites were found on the
566 surfaces. Figures 7b - e showed the surface morphology of the aspirin loaded wafers (samples
567 DL1, DL2, DL8, DL13 and DL14 respectively. These DL wafers showed a very compact
568 polymer matrix structure with crystals of aspirin distributed over their surfaces. Compared to
569 the BLK wafers (samples B2 and C2), the corresponding DL wafers showed lower porosity
570 with smaller more compact pores, which confirms the % swelling capacity (section 3.3 and
571 porosity (section 3.5) results. The very small pores arose because of thicker wall formed
572 which was attributed to polymer-drug interaction.
573
574 *3.5 Pore analysis*
575 Figure S3 (supplementary data) shows the porosity (%) of MET:CAR and MET:CS
576 wafers relative to total polymer content in the original gels and polymer ratios. The results
577 demonstrated a decrease in porosity as MET concentration increased in MET:CAR wafers.
578 However, with the MET:CS formulations, porosity (%) increased slightly with total polymer
579 concentration and with decreased ratio of MET in the formulations. The highest porosity (%)
580 values were for MET:CAR wafers were observed for MET:CAR 1:1 (samples B1 and B2)
581 with values of 98 ± 7% and 96 ± 5%, respectively. For MET:CS wafers the two formulations
582 that showed highest porosity were samples E2 and F2 (MET:CS ratio 1:1 and 3:1) with
583 values of 98 ± 12% and 100 ± 8%, respectively. The lower porosity values for MET:CAR

584 formulations can be attributed to collapsed pore capillaries which were observed in SEM
585 (section 3.4) and thus solvent could not penetrate very well to hydrate the matrix. It was also
586 observed that for MET:CAR the porosity was decreased at higher concentration of total
587 polymer due to the increased crosslink density. As described in the SEM (section 3.4), the
588 MET:CS wafers were more brittle in appearance compared with MET:CAR which could be
589 attributed to the presence of sub pores, thus facilitating the penetration of the solvent into the
590 wafers and producing higher porosity % values.

591 Figure S4 (supplementary data) shows the porosity (%) of DL MET:CAR (samples
592 DL1 and DL2) wafers. It can be observed that as the concentration of MET increased in the
593 formulations the porosity % also increased. However, with the CAR:CS 1:1 formulations
594 (sample DL14), porosity % of the wafers decreased with increase of CS in the formulation
595 from 68.76 ± 8.54 for sample DL14 to 58.22 ± 7.46% for CAR:CS 1:3 (sample DL13). The
596 highest porosity % of the DL wafers were observed for MET:CAR 3:1, 1:1 (samples DL1,
597 DL2) and MET:CS ratio 1:3 (sample DL8) which demonstrated porosity values of 82.45 ±
598 12.39, 70.82 ± 2.30 and 75.11 ± 6.52% respectively. Generally, the porosity in DL wafers
599 was less than the corresponding BLK wafers, which might be due to blockage of some
600 capillaries which slowed down solvent penetration within the DL wafers and confirms the
601 SEM observations.

602

603 *3.6 X-ray powder diffraction*

604 Figure 8a shows the transmission diffractograms of pure starting materials (MET, CS,
605 CAR and aspirin). The results confirms the amorphous nature of MET with a broad peak at
606 2θ 10° and 20°, whilst CS also showed the broad peak at 2θ 12° and 25°. CAR confirmed an
607 amorphous nature with the presence of additional small crystalline sharp peaks at 2θ of 28°,

608 40° attributed to inorganic salt impurities from KCl (Prasad, et al., 2009). Aspirin showed its
609 crystalline nature with the presence of sharp peaks at 2θ of 15°, 20°, 23° and 27°.
610 Figures 8b shows the transmission diffractograms of representative BLK MET:CAR
611 1:1 and 3:1wafers (samples B1, C1, B2 and C2) with no loaded drug BLK. Figure 8c shows
612 the transmission diffractograms of BLK MET:CS 1:1 and 3:1 wafers (samples E1, F1, E2 and
613 F2), The diffractogram confirms the amorphous nature of the samples similar to the pure
614 starting polymers, however, peaks at 2θ 18°, 40°, 50°, 60° and 68° were observed and
615 attributed to inorganic KCl salt impurities present in CAR as well the presence of a broad
616 amorphous peak at 2θ 10° and 20° attributed to MET. A small crystalline shoulder peak at 2θ
617 of 23° was observed for the MET:CAR 3:1 and 1:1 wafers (sample C2 and B2), which could
618 be attributed to false peak detection arising from compression of the wafer which causes the
619 leafy networks to be assembled on top of each other and detected as a false crystalline peak
620 (Okeke & Boateng, 2016). Although it is well known that the amorphous forms are generally
621 unstable and have the tendency to convert back to more stable crystalline forms, they have
622 the advantage of higher solubility and therefore higher rates of dissolution which enhance
623 drug release, absorption and bioavailability. During swelling, amorphous formulations can
624 absorb more dissolution medium and so the diffusion and the release of the drug can be
625 accelerated.
626 Figure 9 shows the XRD diffractograms of DL formulations; MET:CAR 1:1 and 3:1
627 (samples DL1, DL2), CAR:CS 1:1 and 1:3 (DL14, DL13) and MET:CS 1:3 (sample DL8)
628 wafers. The crystalline peaks from aspirin can be observed in all the DL wafers at the same
629 2θ positions of 15°, 20°, 23° and 27° as shown for the pure drug. Further new crystalline
630 peaks were formed with the addition of aspirin in the BLK formulations attributed to
631 alterations within the amorphous polymers, suggesting possible drug-polymer interaction as
632 previously reported (Haeria, et al., 2015). The results suggest that the high aspirin loaded

remained largely in the crystalline form and not molecularly dispersed within the polymer matrix or converted to the amorphous form, and this is expected to enhance its stability in terms of polymorphic transformation.

3.6 Attenuated total reflectance Fourier transform infrared spectroscopy (ATR-FTIR) analysis

As infrared radiation interacts with the bonds between the atoms of a molecule, it is a good technique to investigate functional groups and their interactions within formulations. Figure 10a shows the ATR-FTIR spectra of pure MET, CAR, and CS. The bands at 1223 cm^{-1} and 843 cm^{-1} were attributed to O-S-O symmetric vibration and the band at 925 cm^{-1} demonstrated the existence of C-O-C of the 3,-anhydro-D-galactose for CAR. It also showed bands around 3389, 1036 cm^{-1} which were attributed to O-H and C-O stretches. The intense band at 1625 cm^{-1} was related to water deformation. In the case of MET there was a band around 3444 cm^{-1} which correlates to the O-H stretch, an intense band around 1451 cm^{-1} corresponding to the symmetric vibration of COO, an absorption peak at 2896 cm^{-1} related to C-H stretch, the 1053 cm^{-1} related to C-O stretch and 945 cm^{-1} corresponding for C-O-C. CS showed a peak at 2877 cm^{-1} corresponding to C-H stretch, an intense band at 1607 cm^{-1} corresponding to water deformation, a peak at 1059 cm^{-1} that relates to O-H stretch and 1376 cm^{-1} related to the symmetric vibration of COO. Figure 10a also shows the IR spectra of aspirin which has three functional groups, a benzene ring (aromatic group), a carboxylic acid (COOH) group and an ester (R-C=O-O-R) group. The broad and wide peak from 2500 to 3300 cm^{-1} represents the carboxylic acid (COOH) part of the molecule. The aromatic functional group is represented by the sharp peak for the C-H stretch around 1710-1780 cm^{-1}, a medium peak around 1500-1700 cm^{-1} and a carbonyl group C=O group stretch around 1710-1780 cm^{-1}. The ester group is represented by a C=O stretch at 1735-1750 cm^{-1}.

658 The drug loaded wafers represented in [(Figure S2) supplementary data] shows the
659 interaction of aspirin with the polymers by the broad peak around 2500 cm^{-1} to 3300 cm^{-1}
660 representing the COOH group. This interaction is shown by the shifting of the peaks to a high
661 wavenumber and the reduced peak intensity between 1710 – 1780 cm^{-1} (aromatic group) of
662 aspirin. The bands at 1223 cm^{-1} and 843 cm-^{1} were attributed to O-S-O symmetric vibration
663 and the band at 925 cm^{-1} demonstrated the existence of C-O-C of the 3,-anhydro-D-galactose
664 for CAR. It also showed bands around 3389, 1036 cm^{-1} which were related to O-H and C-O
665 stretch. The intense band at 1625 cm^{-1} was related to the deformation of hydrogen bond in
666 water and described as water deformation band.
667
668 *3.7 Thermogravimetric analysis (TGA)*
669 Table 3 shows the TGA results for both pure starting polymers and the selected
670 optimized composite BLK composite wafers. The pure compounds were analyzed up to 600
671 °C and showed a degradation point at around 250 °C, therefore the wafers were analyzed up
672 to 250 °C. Amorphous polymers which contain water molecules that are bonded to monomer
673 chains or units have an impact on their glass transition temperature and these polymers
674 usually undergo spontaneous transformation towards low energy equilibrium states. This is
675 usually described as relaxation phenomena which indicates structural changes in the materials
676 and affects other properties such as mechanical properties. The results showed that the
677 wafers prepared from MET:CAR 1:1 wafers (samples B1 and B2) had higher residual water
678 than MET:CAR ratio 3:1 wafers (samples C1 and C2), which is due to the higher ratio of
679 MET present in samples C1 and C2 which had a very low residual water of 4.53%. Similar
680 results were demonstrated with MET:CS 3:1 wafers (samples F1 and F2), which showed
681 lower residual water compared to MET:CS 1:1 (samples E1 and E2), which may be attributed
682 to the amount of MET in the formulation. Keeping an adequate amount of residual moisture

683 content within the wafers was vital as lower water content reduces molecular mobility and
684 increases shelf-life by avoiding earlier hydration of the active drug (Rodriguez-Spong, et al.,
685 2004). An acceptable residual moisture is required for these formulations as the target drug,
686 aspirin, is unstable in water due to hydrolysis. The loss of weight observed for all samples
687 during heating stage occurred between 60 °C and 120 °C and is an indication of the fact that
688 weight loss was due to bound water (Chen & C, 1999).
689 As seen in table 3 lower amounts of residual water were observed in the DL wafers.
690 The amount of water present in the DL wafers was of 3.92, 3.97, 5.88 and 7.15 % for the
691 wafers prepared from MET:CAR ratio 1:1 and 3:1, CAR:CS 1:3 and MET:CS 1:3 (samples
692 DL1, DL2, DL13, DL14 and DL8) respectively. The % weight loss after 150 °C was
693 attributed to possible degradation of aspirin and these results helped to inform the DSC
694 settings and the maximum temperature of 150 °C for the DL wafers was selected in order to
695 limit possible aspirin degradation.
696
697 *3.8 Differential scanning calorimetry (DSC)*
698 DSC was used to define the possible interactions between the materials within the selected
699 optimized wafers matrix. (Table 4) shows the main DSC thermal transitions observed from
700 the thermograms of pure MET, CAR and CS all of which showed broad endothermic peaks at
701 69.72 °C, 95.08 °C and 89.54 °C respectively. The BLK wafers also showed broad
702 endothermic peaks at 74.53 °C, 65.27 °C and 70.39 °C for the wafers prepared from
703 MET:CAR ratios 1:1, 3:1 (samples B2, C2) and MET:CS 1:1 (sample E2) respectively. These
704 peaks can be attributed to water evaporation as noted by Neto and co-workers, who observed
705 that water peaks usually fall in the range of 50-150 °C (Neto, et al., 2005). Even though a
706 heat-cool-heat cycle (involving heating the sample to the highest temperature (200 °C)
707 without degrading, removing all residual moisture, cooling it down to the starting temperature

(-50 °C) and then heating again to (200 °C) was used, there was no glass transition observed thermograms in any of the pure materials, BLK and DL wafers which is attributed to possible suppression by the endothermic peak from water evaporation (Yoshida, et al., 1992). The DSC results for the pure polymers and BLK wafers showed that the formulations can be considered as amorphous because no melting peak was not observed in the thermograms of the wafers and it is confirmed by the XRD spectrograms on section 3.6.

DSC was also used to determine the possible interactions between polymers in the composite MET:CAR 3:1, 1:1, CAR:CS 1:3, 1:1 and MET:CS 1:3 wafers (samples DL1, DL2, DL13, DL14 and DL8) and model drug (aspirin) and also confirm their physical form. Table 4 also shows the DSC profiles of aspirin and representative DL MET:CAR, MET:CS and CAR:CS wafers. The pure aspirin showed a sharp endothermic peak at 141.94 °C, indicating melting point of the drug. Aspirin could not be analyzed beyond 160.00 °C for a re-crystallization peak after melting due to possible aspirin degradation as depicted in the TGA analysis. Though there was no glass transition peaks in the DL wafers thermograms (as was the case in the BLK wafers), they all showed melting transition peaks which were slightly broader than the pure aspirin peak. It can be observed that the melt peak of the DL wafers shifted from 141.94 °C to a lower temperature of 124.48 °C, 130.68 °C and 131.21 °C for the DL wafers prepared form MET:CAR 3:1, CAR:CS 1:3 and MET:CS 1:3 (samples DL1, DL13 and DL8) respectively. This is attributed to physical mixing and interaction of the aspirin within the polymer matrix confirmed by the FTIR results in section 3.6 which showed that aspirin interacted with the polymers.

3.9 In vitro drug release

Drugs can be released from polymer matrix by diffusion through the swollen polymer and subsequent erosion of the matrix. The drug release may be controlled by diffusion, or by a

combination of diffusion and erosion or only by erosion of the delivery system (Khan, et al., 2016). Before the drug dissolution studies, the drug loading (assay) in each wafer sample was determined using SS and PBS. The dissolution profile (figure 11a) for DL wafers in PBS solution pH 6.8 ± showed that during the early stage of dissolution there was an almost linear release profile, which was confirmed by fitting the data to Korsmeyer-Peppas equation, (supplementary data section S1, table S2). It was observed that for the MET:CAR 1:1 and 3:1 wafers (samples DL1 and DL2) the release was 70.8 % and 63.3 % respectively within 20 minutes. For the CAR:CS 1:1 (sample DL14) the release of the drug was 64.8 % within 20 minutes and for CAR:CS 1:3 (sample DL13) the release was of 90.5 % within the same time period. The release of MET:CS (sample DL8) was of 100.0 % within 20 minutes.

The dissolution profile of DL wafers were also observed in (figure 11b) using SS at pH 6.8 ± 0.1. The SS helps to accurately mimic the environment of the oral cavity such as pH and ionic strength. The % release was observed to be lower than in PBS with only 41.9 % released for MET:CAR 1:1 (sample DL1) and 42.8% for MET:CAR 3:1(sample DL2). For the CAR:CS 1:3 wafers (samples DL13), 20.0 % was released in the first 20 minutes and gradually increased to 32.9 % at 60 minutes and 42.0% at 90 minutes and then remained fairly constant till 120 minutes.

Though the DL wafers appeared to show some controlled release in the two dissolution media over 2 hours, PBS showed higher cumulative release than SS which is related to the effect of SS on the initial swelling of the polymer matrix and subsequent drug diffusion as well as matrix erosion. The drug release was faster in PBS than in SS due to the difference in osmotic pressure and ionic strength as SS contains more sodium, chloride and sulfate ions than PBS. It was observed that the formulations with lower swelling capacity, which disintegrated within 2 to 30 minutes CAR:CS 1:1 and 1:3 (samples DL14, DL13) and MET:CS 1:3(sample DL8)) showed a higher release profile than MET:CAR 1:1 and 3:1 the

formulations (samples DL1 and DL2) which correlated very well with the swelling capacity data described in section 3.3.

Wafers prepared from MET:CAR 3:1 (sample DL1) had a lower release compared to sample DL2 which is due to the increased MET in the formulations which helps to increase the viscosity and density of the wafers thus controlling drug diffusion and release. This was also observed in swelling capacity where sample DL2 showed a higher swelling capacity and also due to higher porosity which allowed more media to penetrate the polymeric matrix as was observed in section 3.3.7.

Overall, the drug release profiles shows the formulations fall into two distinct categories with the DL MET:CAR formulations showing relatively slower drug release due to their swelling nature due to the presence of MET, whilst the CAR:CS formulations generally disintegrated rapidly upon contact with dissolution medium and consequently releasing the contained drug relatively quickly. This will suggest that once applied in the oral cavity, the two formulations will behave differently with the CAR:CS wafers most likely disintegrating rapidly into a free flowing gel that will be swallowed for gastric absorption. On the other hand the MET:CAR wafers will most likely remain in the oral cavity including the buccal mucosa, long enough to allow pre-gastric absorption through the buccal mucosa and subsequently swallowing of the remaining dose present in saliva. However, this will need to be further investigated in an in vivo study.

4.0 Conclusion

Composite MET:CAR and CAR:CS and MET:CS loaded with aspirin have been successfully formulated as potential oral and buccal delivery systems for low dose aspirin. The use of composite polymeric systems was implemented to increase the functional properties of the polymeric dosage forms. The results demonstrated that mucoadhesion, physico-characteristics, swelling capacity and microscopic structure were influenced by higher

783 concentration of MET and the total amount of total polymer weight which increased the
784 density of the formulations. The DL wafers did not show highly porous internal morphology,
785 instead they showed very small pores in a thick walled matrix due to polymer-drug
786 interactions. . The aspirin was released much faster in PBS than in SS which is attributed to
787 the matrix of polymeric wafers and interactions with the two media as a result of the
788 differences in ionic strength. By fitting the dissolution data for PBS and SS into Korsmeyer-
789 Peppas equation, it was concluded that the drug release were controlled by diffusion or by
790 combination of diffusion and erosion depending on the formulation composition and ionic
791 environment (PBS or SS). Wafers prepared from MET:CAR 1:1 and 3:1 (samples DL2 and
792 DL1) and CAR:CS 3:1 and 1:1 (samples DL13 and DL14) and MET:CS 3:1 (sample DL8)
793 loaded with 75 mg aspirin are good candidates for the delivery of low dose aspirin for the
794 elderly people, based on visual and physico-chemical characterization. Based on the swelling
795 and drug dissolution results, The MET:CAR 3:1 wafer (DL1) with longer swelling time could
796 be used for controlled release of aspirin via the buccal mucosa (pregastric absorption), whilst
797 CAR:CS 1:1 wafer (DL14) can be used as a fast disintegrating delivery system that will
798 combine initial buccal (pregastric) absorption and subsequent GIT (gastric) absorption
799 swallowing the remaining free flowing gel.
800
801 **Conflict of interest**
802 The authors report no conflict of interest.
803
804 **References**
805 Ayensu, I., Mitchell , J.C., Boateng, J. S. 2012. Development and Physico-mechanical
806 Characterisation of Lyophilised Chitosan Wafers as Potential Protein Drug Delivery Systems
807 via the Buccal Mucosa. Coll. Surf. B: Biointerf. 91, 258-265.

808 Boateng, J.S., Ayensu, I. 2014. Preparation and characterization of laminated thiolated
809 chitosan-based freeze-dried wafers for potential buccal delivery of macromolecules, Drug
810 Dev. Ind. Pharm. 40 (5), 611-618.

811 Boateng, J.S., Auffret, A.D., Matthews, K.H., Humphrey, M.J., Stevens, HN., Eccleston,
812 G.M. 2010. Characterisation of freeze-dried wafers and solvent evaporated films as potential
813 drug delivery systems to mucosal surfaces. *International Journal of Pharmaceutics*, 389; 24–
814 31.

815 Boateng, J. S., Ayensu, I. 2014. Preparation and characterisation of laminated thiolated
816 chitosan-based freeze-dried wafers for potential buccal delivery of macromolecules. Drug
817 Dev. Ind. Pharm. 40(5), 611-618.
818 British Medical Association , 2014. Aspirin to prevent blood clots. British Medical
819 Association and Royal Pharmaceutical Society.
820 Campo, V. L., Kawano, D. F., da Silva Jr, D. B. Carvalho, I., 2009. Carrageenans: Biological
821 properties, chemical modification and structural analysis - A review. Carbohydr. Polym. 77,
822 167-180.
823 Chen, L.L., Chetty, D.J., Chien, Y.W. 1999. A mechanistic analysis to characterize
824 oralmucosal permeation properties. Int. J. Pharm.184(1), 63-72.
825 Haeria, A., Nisaa, N., Isriany, I. 2015. Characterization and dissolution test of aspirin-
826 nicotinamide cocrystal. Int. J. Pharm. Tech. Res. 8(1), 166-170.
827 Hitesh, V. C., Rupal, D. P., Ishan , P. M., Chhagan, N. P. 2012. Preparation and
828 characterization of superporous hydrogel based on different polymers. Int. J. Pharm. Investig.
829 2(3), 134-139.
830 Khan, S., Boateng, J.S., Trivedi, V., Mithcell, J. 2015. Formulation, characterization and
831 stabilization of buccal films for pediatric drug delivery of omeprazole. AAPS PharmSciTech,
832 16(4), 500-510.

833 Khan, S., Trivedi, V. & Boateng, J., 2016. Functional physico-chemical, ex vivo permeation
834 and cell viability characterisation of omeprazole loaded buccal films for paediatric drug
835 delivery. Int. J. Pharm. 500, 217-226.
836 Kianfar, F., Antonijevic, M. D., Chowdhry, B. Z. & Boateng, J.S. 2011. Formulation
837 Development of a Carrageenan Based Delivery System for Buccal Drug Delivery Using
838 Ibuprofen as a Model Drug. J. Biomater. Nanobiotech. 2, 528-595.
839 Kianfar, F., Ayensu, I., Boateng, J.S. 2014. Development and physico-mechanical
840 characterization of carrageenan and poloxamer-based lyophilized matrix as a potential buccal
841 drug delivery system. Drug Dev. Ind. Pharm. 40 (3), 361-369.
842 Lefnaoui, S., Moulai-Mostefa, N. 2011. Formulation and in vitro evaluations of kappa-
843 carrageenan-pregelatinised starch-based mucoadhesive gels containing miconazole. Starch-
844 Starke. 63(8), 512-521.
845 Marques, M.R.C., Loebenberg, R., Almukainzi, M. 2011. Simulated Biological Fluids with
846 Possible Application in Dissolution Testing. Dissol. Technol. 18(3), 15-28.
847 Neto, C.G.T., Giacometti, J.A., Job, A.E., Ferreira, F.C., Fonseca, J.L.C., Pereira, M.R. 2005.
848 Thermal analysis of chitosan based networks. Carbohydr. Polym. 62(2) 97-103.
849 Nireesha, G.R., Divya, L., Sowmya, C., Venkateshan, N., Niranjan Babu, M., Lavakuma, V.
850 2013. Lyophilisation/Freze drying - A Review. Int. J. Novel Trends Pharm. Sci. 3(4), 87-98.
851 Okeke, O.C., Boateng, J.S., 2016. Composite HPMC and sodium alginate based buccal
852 formulations for nicotine replacement therapy. Int. J. Biol Macromol. 91, 31-44.
853 Okeke, O.C., Boateng, J.S. 2017. Nicotine stabilization in composite sodium alginate based
854 wafers and films for nicotine replacement therapy. Carbohydr. Polym. 155, 78-88.
855 Pairatwachapun, S., Paradee, N. Sirivat, A. 2016. Controlled release of acetylic acid from
856 polythiophene/carrageenan hydrogel via electrical stimulation. Carbohydr. Polym. 137, 214-
857 221.

858 Panda, B., Dey, N., Rao, M. 2012. Development of Innovative Orally Fast Disintegrating
859 Film Dosafe Forms: A Review. J. Pharm. Sci. Nanotech. 5(2), 1666-1674.
860 Parkash, V., Deepka S.M., Yadav, S.K., Jogpal H.V. 2011. Fast Disintegrating Tablets:
861 Opportunity in Drug Delivery System. J. Adv. Pharm. Tech. Res. 2(4), 223-235.
862 Park, H., Robinson, J.R. 1985. Physico-chemical properties of water insoluble polymers
863 important to mucin/epithelial adhesion. J. Contr. Rel. 2, 47-57.
864 Peh, K.K., Wong, C.F. 1999. Polymeric Films as Vehicle for Buccal Delivery: Swelling,
865 Mechanical and Bioadhesive Properties. J. Pharm. Pharm. Sci. 2, 53-91.
866 Peh, K.K., Wong, C.F. 1999. Polymerics films as vehicle for buccal delivery: swelling,
867 mechanical and bioadhesive properties. J. Pharm. Pharm. Sci. 2, 53-91.
868 Prasad, K., Kaneko, Y., Kadokawa, J. 2009. Novel gelling systems of kappa-, iota- and
869 lambda-carrageenans and their composite gels with cellulose using ionic liquid. Macromol.
870 Biosci. 9(4), 376-382.
871 Rodriguez-Spong, B., Price, C.P., Jayasankar, A., Matzger, A.J., Rodriguez-Hornedo, N.
872 2004. General principles of pharmaceutical solid polymorphism: a supramolecular
873 perspective. Adv. Drug Del. Rev. 56(3), 241-274.
874 Sattar, M., Sayed, O.M., Lane, M.E. 2014. Oral Transmucosal Drug Delivery Current Status
875 and Future Prospects. Int. J. Pharm. 471, 498-506.
876 Shin Etsu Chemical, 2005. *Metolose,* s.l.: Shin Etsu Chemical Co., Ltd.
877 Shojaei, A.H. 1998. Buccal Mucosa as a Route for Systemic Drug Delivery: A Review. J.
878 Pharm. Sci. 1(1), 15-30.
879 Siriwat, T., Chowwanapoonpohn, S., Okonohi, S., Yotsawimonwat, S. 2012. Solubility,
880 Viscosity and Rheological Properties of Water Soluble Chitosan Derivatives. Maejo Int. J.
881 Sci. Tech. 6(2), 315-322.

882 Smart, J., 2005. The basics and underlying mechanisms of mucoadhesion. Adv. Drug Del.
883 Rev. 57, 1556-1565.
884 Sriamornsak, P., Wattanakom, N., Nunthanid, J., Puttipipatkhachorn, S. 2008. Mucoadhesion
885 of pectin as evidence by wettability and chain interpenetration. Carbohydr. Polym. 74(3),
886 458-467.
887 Stanley, N. 2010. Production, Properties and Uses of Carrageenan, Rockland: FMC
888 Corporation, Marine Colloids Division.
889 Tari, O., Kara, S., Pekcan, O. 2009. Critical Exponents of Kappa Carrageenan in the Coil-
890 Helix and Helix Coil Hysteresis Loops. J. Macromol. Sci. Part B: Phys. 48(4), 812-822.
891 Theodorakis, M.J., Guodmundsson, A. 2012. Formulations, Packing and Medication
892 Practices, s.l.: EMA Workshop.
893 Thommes, M., Kleinebudde, P. 2006. Use of Kappa- Carrageenan as Alternative Pelletisation
894 Aid to microcrystalline Cellulose in Extrusion/Spheronisations II. Influence of Drug and
895 Filler Type. Eur. J. Pharm. Biopharm. 63(1), 68-75.
896 Yoshida, H., Hatakeyama, T., Hatakeyama, H. 1992. Characterisation of water in
897 polysaccharide hydrogels by DSC. J. Therm. Anal. 40, 483-489.
898 Zia, K.M., Tabasum, S., Nasif, M., Sultan, N., Aslam, N., Noreen, A., Zuber, M. 2017. A
899 review on synthesis, properties and applications of natural polymer based carrageenan blends
900 and composites. Int. J. Biol. Macromol. 96, 282-301.
901
902

Table 1. Polymeric solutions for preparing BLK freeze-dried formulations in H_2O

Sample name	MET (g)	CAR (g)	Polymer ratio	Total excipient content in polymeric solution (% w/v)
Sample A	0.38	1.12	1:3	1.50
Sample B	0.75	0.75	1:1	1.50
Sample C	1.12	0.38	3:1	1.50
Sample A1	0.50	1.50	1:3	2.00
Sample B1	1.00	1.00	1:1	2.00
Sample C1	1.50	0.50	3:1	2.00
Sample A2	0.63	1.87	1:3	2.50
Sample B2	1.25	1.25	1:1	2.50
Sample C2	1.87	0.63	3:1	2.50
Sample name	**MET (g)**	**CS (g)**	**Polymer ratio**	**Total excipient content in polymeric solution (% w/v)**
Sample D	0.38	1.12	1:3	1.50
Sample E	0.75	0.75	1:1	1.50
Sample F	1.12	0.38	3:1	1.50
Sample D1	0.50	1.50	1:3	2.00
Sample E1	1.00	1.00	1:1	2.00
Sample F1	1.50	0.50	3:1	2.00
Sample D2	0.63	1.87	1:3	2.50
Sample E2	1.25	1.25	1:1	2.50
Sample F2	1.87	0.63	3:1	2.50

903

Table 2. Polymeric solutions for preparing DL freeze-dried formulation in 100 ml of 45% v/v ethanolic solution

Sample name	**MET (g)**	**CAR (g)**	**LMW CS (g)**	**Polymer ratio**	**Total excipient content in polymeric solution (% w/v)**
Sample DL1	1.87	0.63	0.00	3:1	2.50
Sample DL2	1.25	1.25	0.00	1:1	2.50
Sample DL3	1.25	0.63	0.63	2:1:1	2.50
Sample DL4	0.63	1.25	0.63	1:2:1	2.50
Sample DL5	0.63	0.63	1.25	1:1:2	2.50
Sample DL6	1.87	0.00	0.63	3:1	2.50
Sample DL7	1.25	0.00	1.25	1:1	4.00
Sample DL8	3.00	0.00	1.00	1:3	4.00
Sample DL9	0.00	1.87	0.63	3:1	2.50
Sample DL10	0.00	0.63	1.87	1:3	2.50
Sample DL11	0.00	1.25	1.25	1:1	2.50
Sample DL12	0.00	3.00	1.00	3:1	4.00
Sample DL13	0.00	1.00	3.00	1:3	4.00
Sample DL14	0.00	2.00	2.00	1:1	4.00

904

Table 3. Weight loss % from TGA analyses of pure compounds, BLK wafers and DL wafers at 120 °C.

Formulations (BLK wafers)/starting materials	**Weight loss %**
Metolose	4.53
Carrageenan	14.5
Chitosan	18.5
Sample E1	11.67
Sample E2	11.59
Sample F1	2.24
Sample F2	8.62
Sample B1	11.50
Sample B2	9.93
Sample C1	8.11
Sample C2	7.57
DL wafers / aspirin	
Aspirin	0.67
Sample DL2	3.92
Sample DL1	3.97
Sample DL13	5.88
Sample DL8	7.15

905

Table 4. Summary of temperature and heat changes observed for the endothermic transition observed during DSC analysis for pure materials, BLK wafers and DL wafers.

Materials / formulations	**Onset °C**	**Peak °C**	**ΔH (J/g)**
	Pure materials		
Metolose	23.57	69.72	89.11
Carrageenan	42.72	95.08	234.50
LMW chitosan	33.67	89.54	329.70
Aspirin	139.08	141.94	170.50
	BLK wafers		
Sample B2	50.07	74.57	247.40
Sample C2	20.21	65.27	154.50
Sample E2	25.63	70.39	199.10
Formulations	**Onset °C**	**Peak °C**	**ΔH (J/g)**
	DL wafers		
Sample DL1	112.95	124.48	103.70
Sample DL13	121.31	130.68	126.60
Sample DL8	122.93	131.21	120.40

906

907

908

909

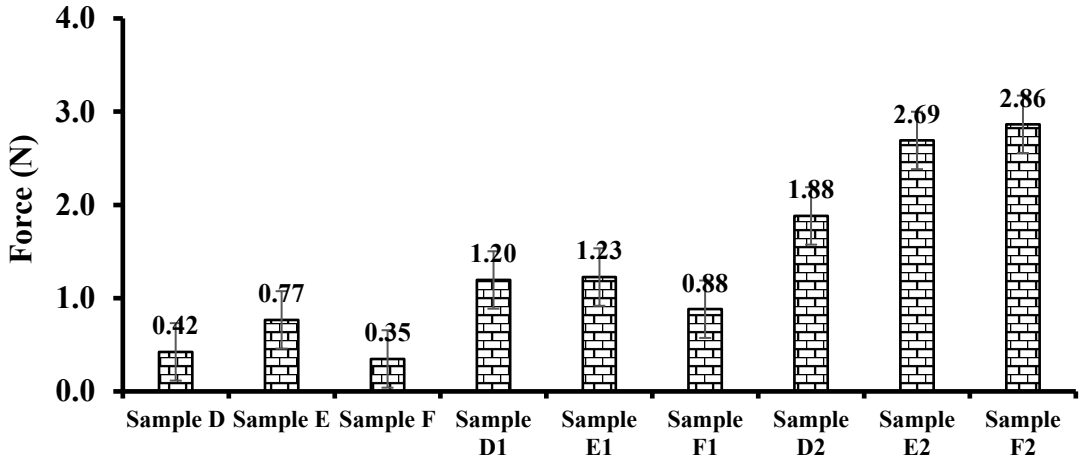

910
911 (a)

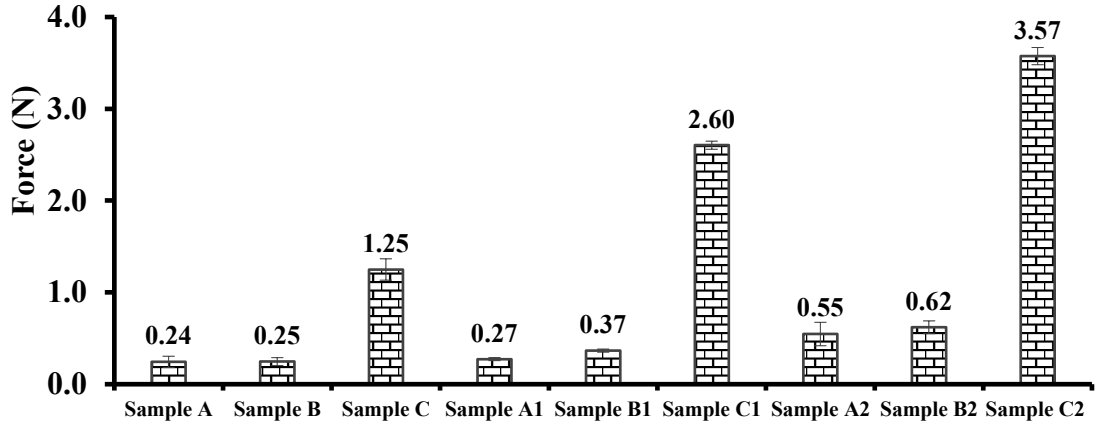

912
913 (b)

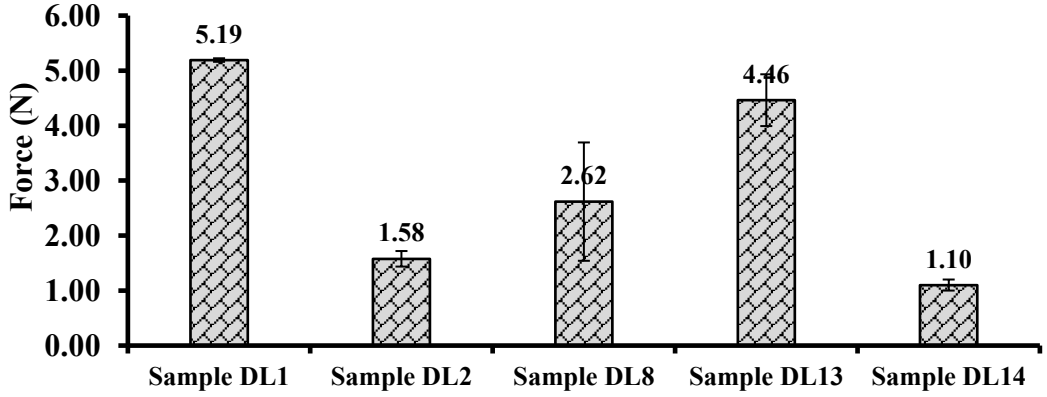

914
915 (c)

916 Figure 1. Resistance to compression (hardness) profiles of BLK composite wafers (a)
917 MET:CS, (b) MET:CAR wafers and (c) DL composite wafers. The test was performed using
918 a Texture Analyser fitted with a 5 kg load cell. Each wafer was compressed in 5 different
919 positions, using a 2mm probe to a depth of 1mm and speed of 1 mm/sec with the instrument
920 in compression mode (mean ± SD, $n = 3$).
921

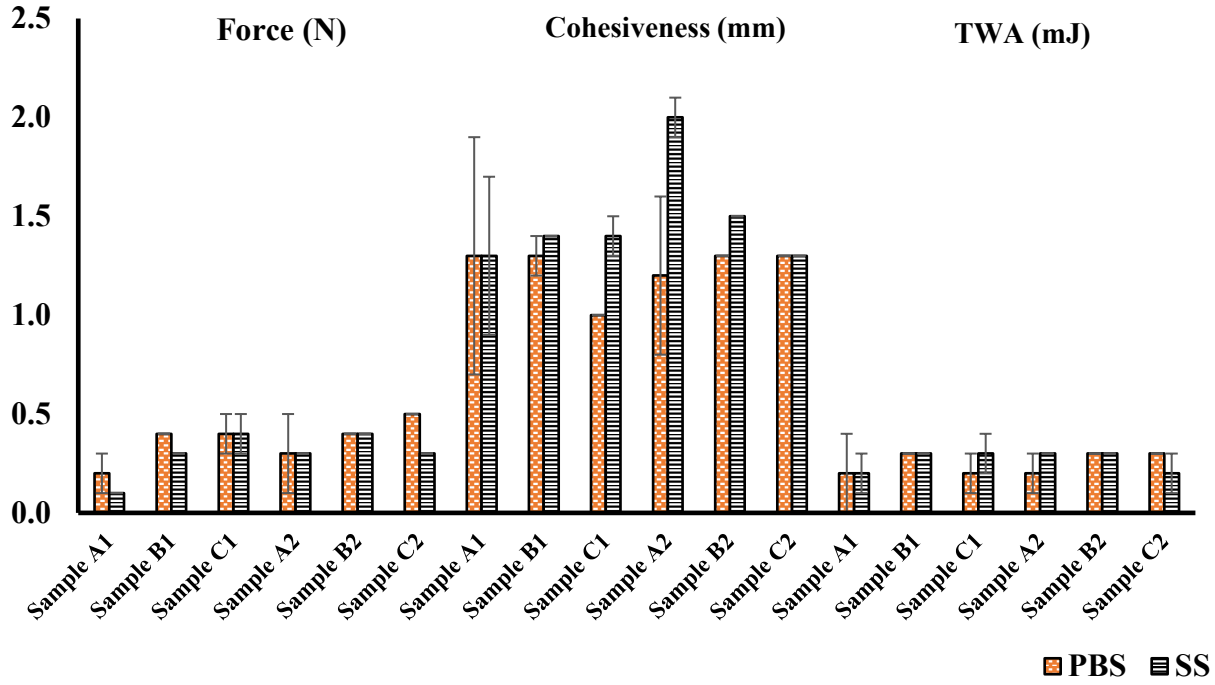

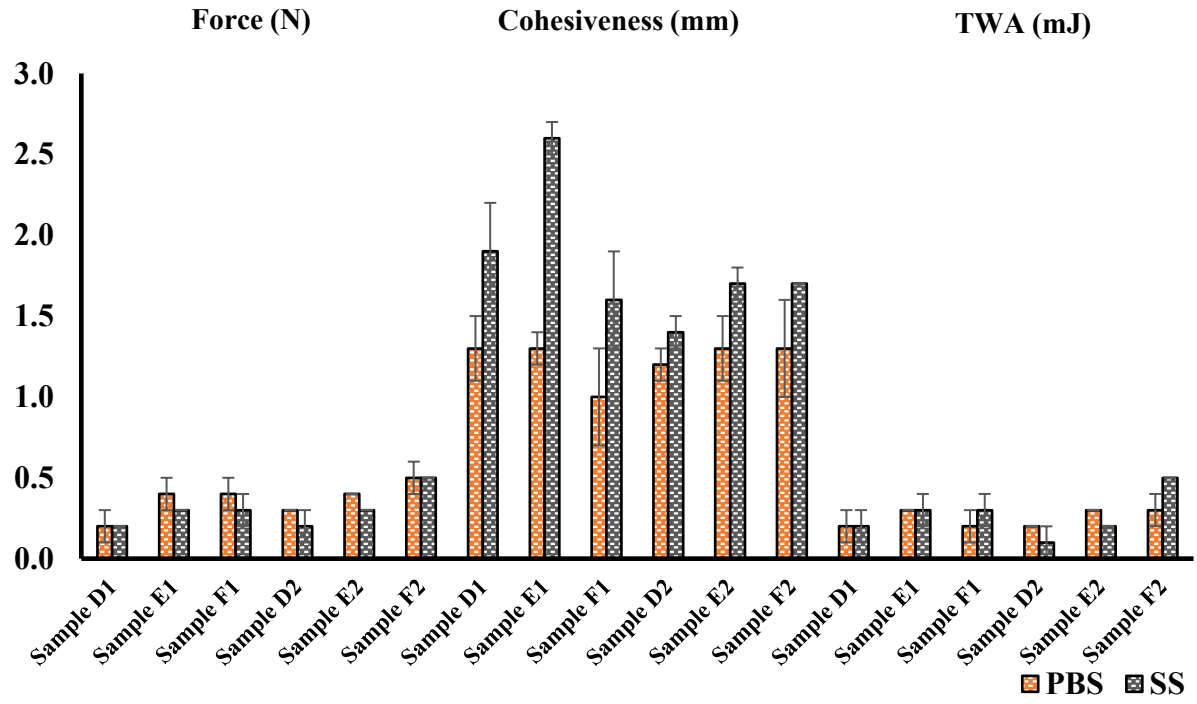

Figure 2. Mucoadhesive profile of BLK composite (a) MET:CAR and (b) MET:CS wafers in SS and PBS . The test was performed using a Texture Analyser fitted with a 5 kg load cell in adhesive mode. The probe with the sample attached was lowered to make contact with the model mucosa surface with an applied force of 1.0 N and was detached after 60 seconds contact. Three replicates were performed for each sample (mean ± SD, n = 3).

930

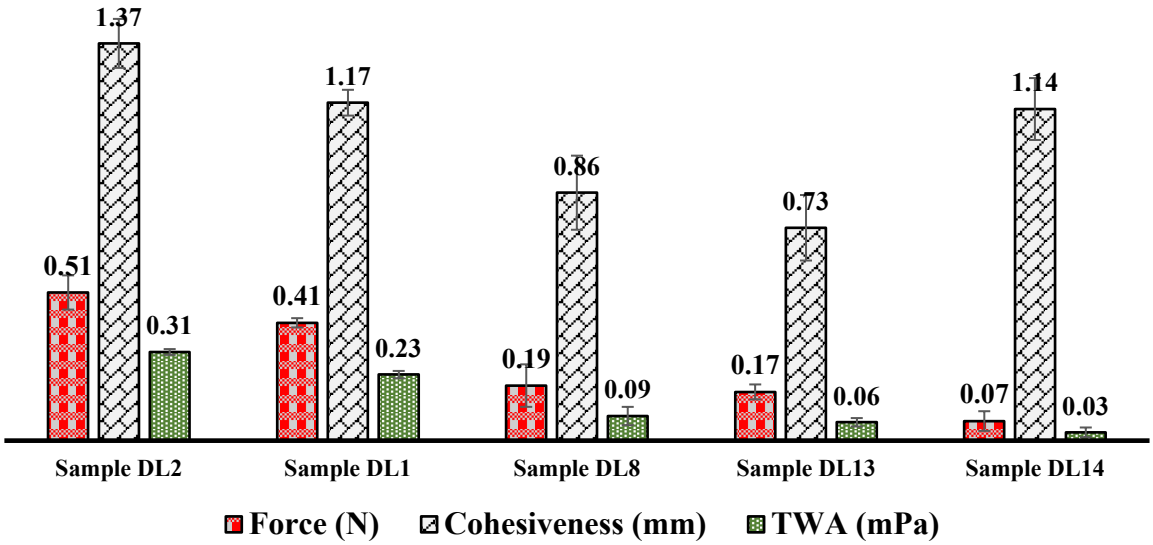

931

932 (a) SS

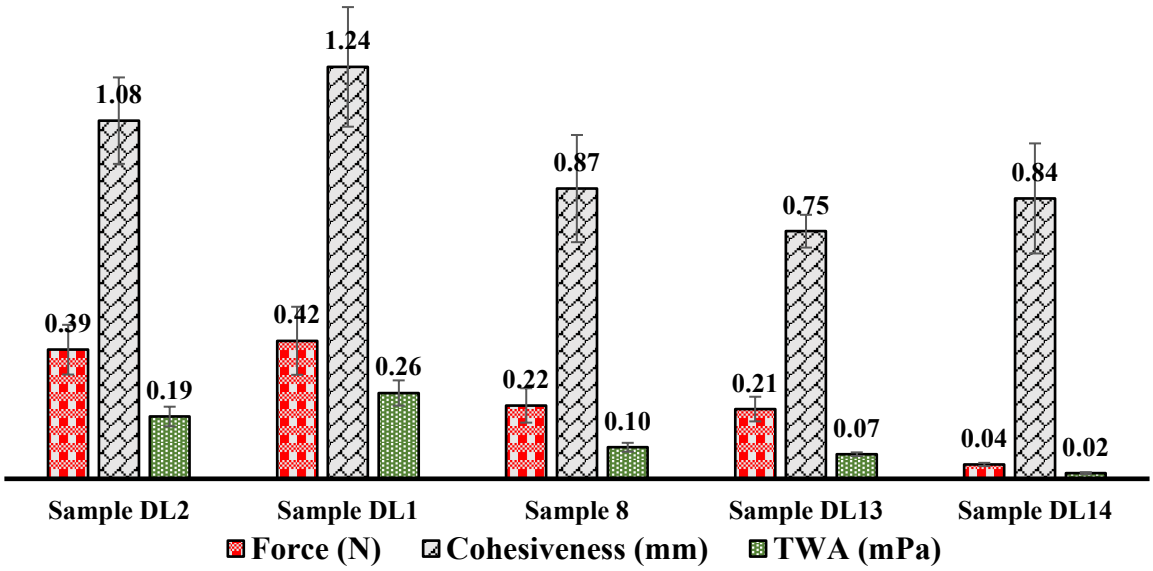

933

934 (b) PBS

935 Figure 3. Mucoadhesion profile of aspirin loaded wafers in (a) SS and (b) PBS. The test was
936 performed using a Texture Analyser fitted with a 5 kg load cell in adhesive mode. The probe
937 with the sample attached was lowered to make contact with the model mucosa surface with
938 an applied force of 1.0 N and was detached after 60 seconds contact. Three replicates were
939 performed for each sample (mean ± SD, n = 3).

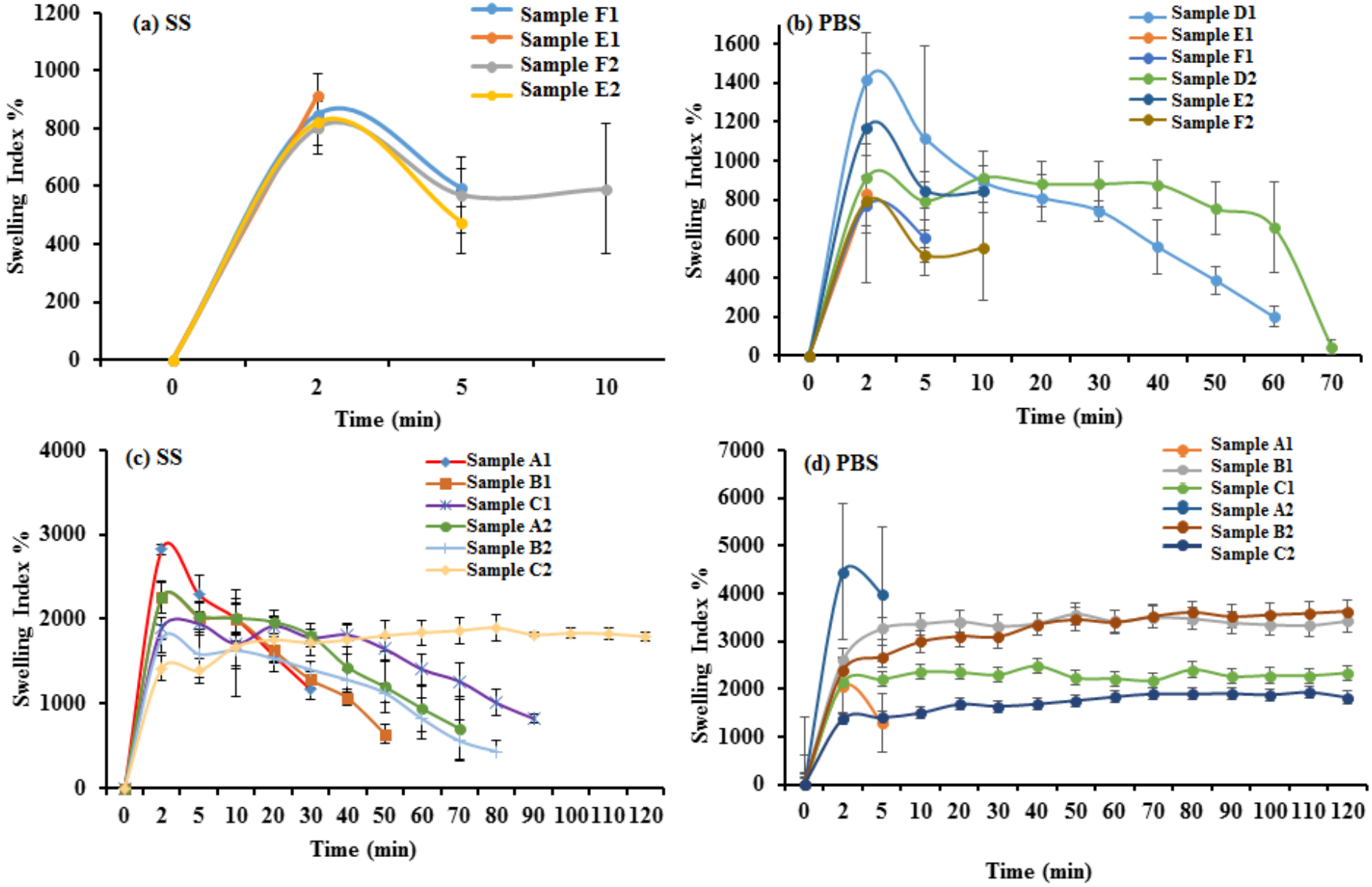
(a) SS
Sample F1
Sample E1
Sample F2
Sample E2
Swelling Index %
Time (min)
(b) PBS
Sample D1
Sample E1
Sample F1
Sample D2
Sample E2
Sample F2
Swelling Index %
Time (min)
(c) SS
Sample A1
Sample B1
Sample C1
Sample A2
Sample B2
Sample C2
Swelling Index %
Time (min)
(d) PBS
Sample A1
Sample B1
Sample C1
Sample A2
Sample B2
Sample C2
Swelling Index %
Time (min)

940

941 Figure 4. Swelling profiles BLK wafers - (a) MET:CS 3:1 and 1:1 (samples E1, F1, E2 and F2) in SS, (b) MET:CS 3:1, 1:1 and 1:3 (samples
942 D1, E1, F1, D2, E2 and F2) in PBS, (c) MET:CAR ratio 1:3, 1:1 and 3:1 (samples A1, B1, C1, A2, B2 and C2) in SS and (d) MET:CAR ratio
943 1:3, 1:1 and 3:1 (samples A1, B1, C1, A2, B2 and C2) in PBS. The swelling capacity was determined at a temperature of 37 ± 0.1°C. It was
944 determined for three replicates (mean ± SD, $n = 3$) and calculated using equation 6.

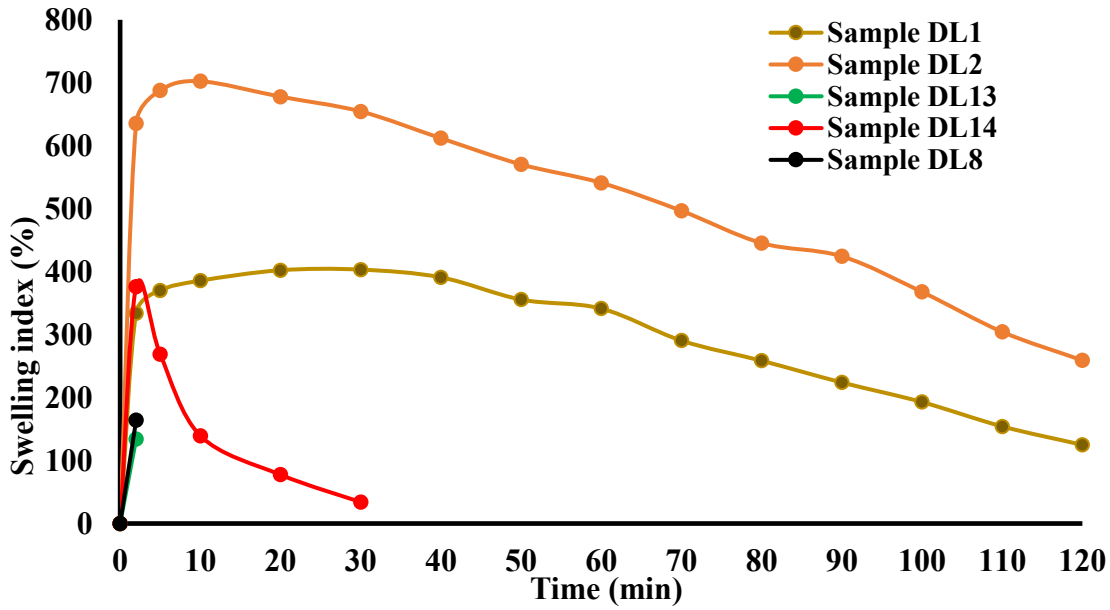

(a) PBS

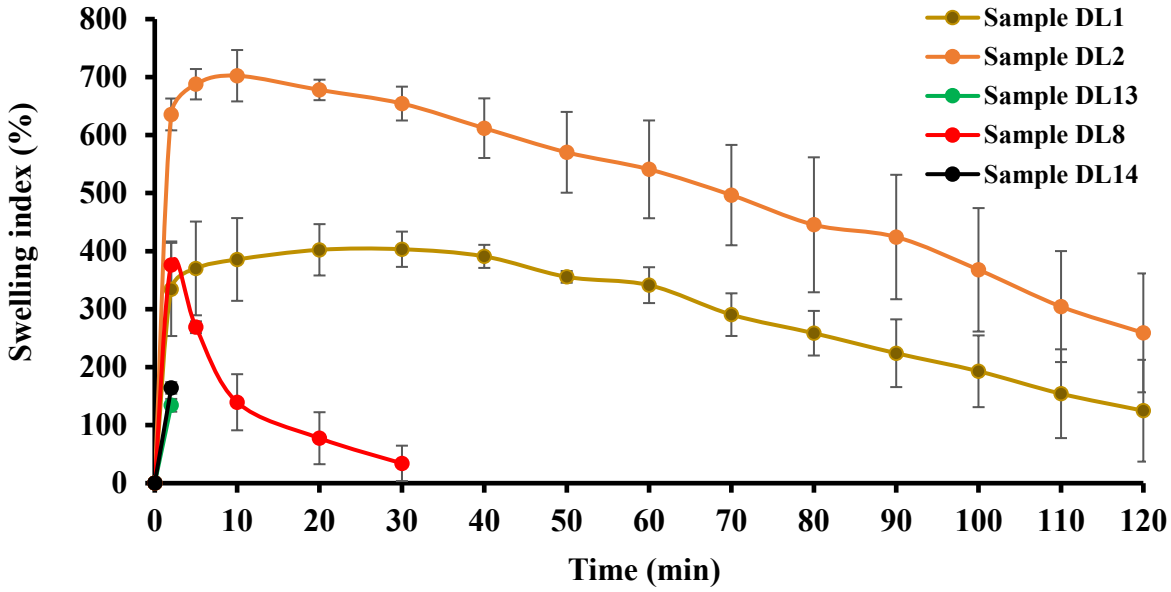

(b) SS

Figure 5. Swelling profiles of DL wafers (a) MET:CAR ratio 1:1, and 3:1 (samples DL2 and DL3), CAR:CS ratio 1:3 and 1:1 (samples DL13 and DL14) and MET:CS ratio 1:3 (sample DL8) in PBS (b) MET:CAR ratio 1:1 and 3:1 (samples DL2 and DL3), CAR:CS ratio 1:3 and 1:1 (samples DL13 and DL14) and MET:CS ratio 1:3 (sample DL8) in SS. The swelling capacity was determined at a temperature of 37 ± 0.1°C. It was determined for three replicates (mean ± SD, n = 3) and calculated using equation 6.

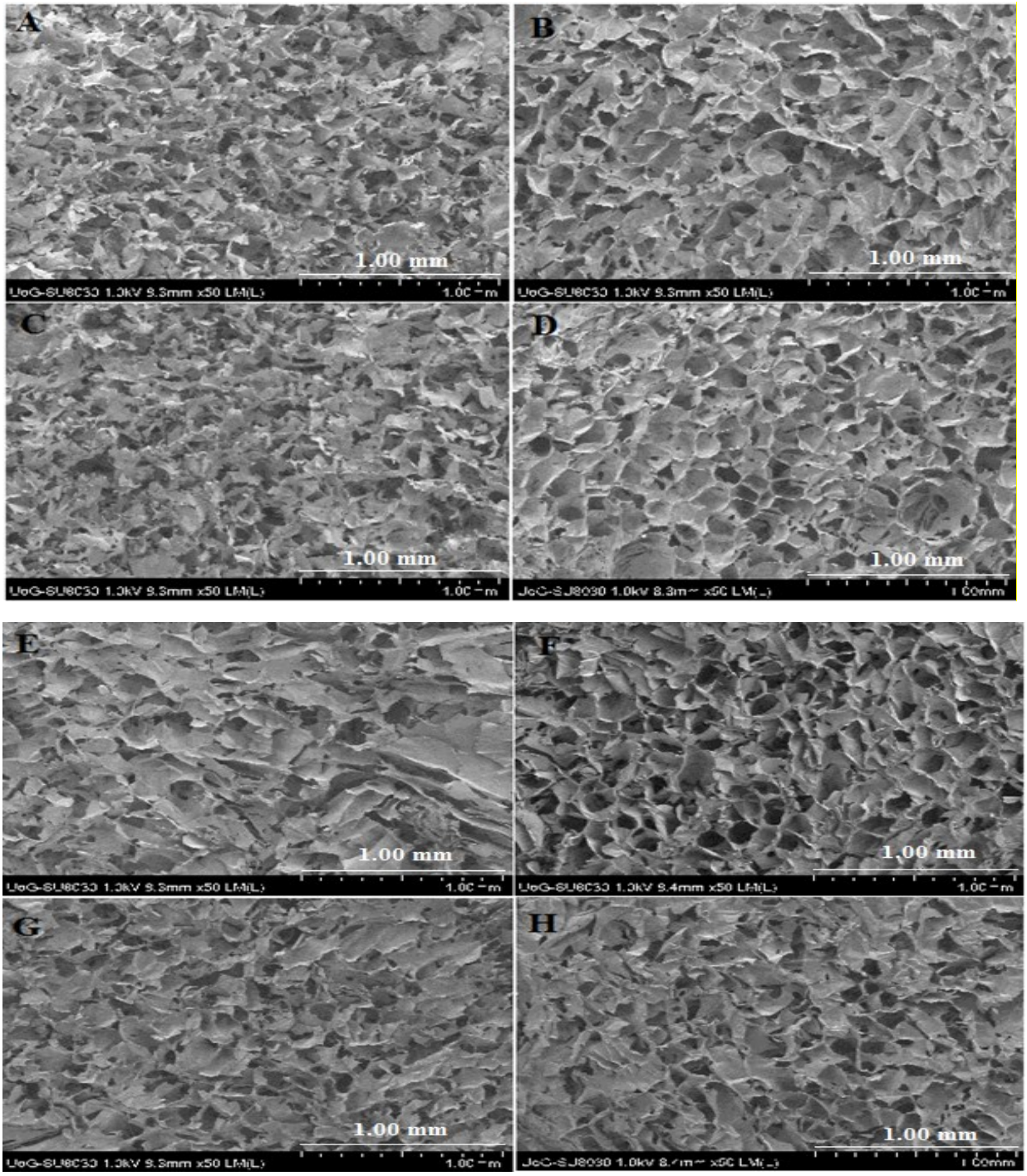

Figure 6. SEM images showing the internal porous structure and surface morphology of the BLK wafers [(a) MET:CAR 1:1 (sample B1) (b) MET:CAR 3:1 (sample C1) (c) MET:CAR 1:1 (sample B2) (d) MET:CAR 3:1 (sample C2) (e) MET:CS 1:1 (sample E1) (f) MET:CS 3:1 (sample F1) (g) MET:CS 1:1 (sample E2) and (h) MET:CS 3:1 (sample F2)]. The surface morphology was analysed using a Hitachi SU8030. The wafers were coated with chromium using a Sputter Coater and analysed at 5.0 kV accelerating voltage.

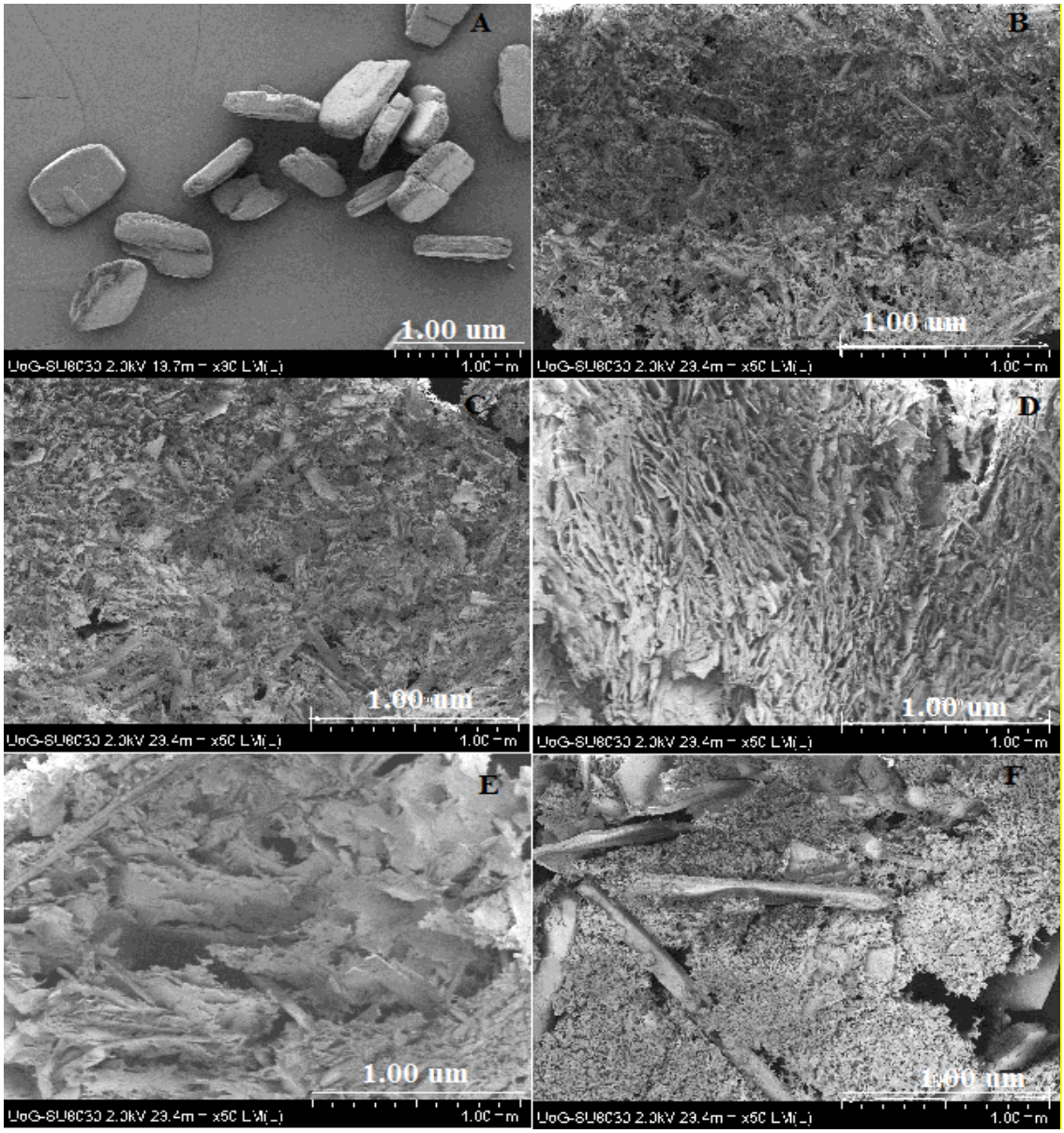

Figure 7. SEM images showing the internal porous structure and surface morphology of the (a) aspirin and DL wafers [(b) MET:CAR 3:1 (sample DL1) (c) MET:CAR 1:1 (sample DL 2) (d) MET:CS 1:3 (sample DL8) (e) CAR:CS 1:3 (sample DL13) and (f) CAR:CS 1:1 (sample DL14)]. The surface morphology was analysed using a Hitachi SU8030. The wafers were coated with chromium using a Sputter Coater and analysed at 5.0 kV accelerating voltage.

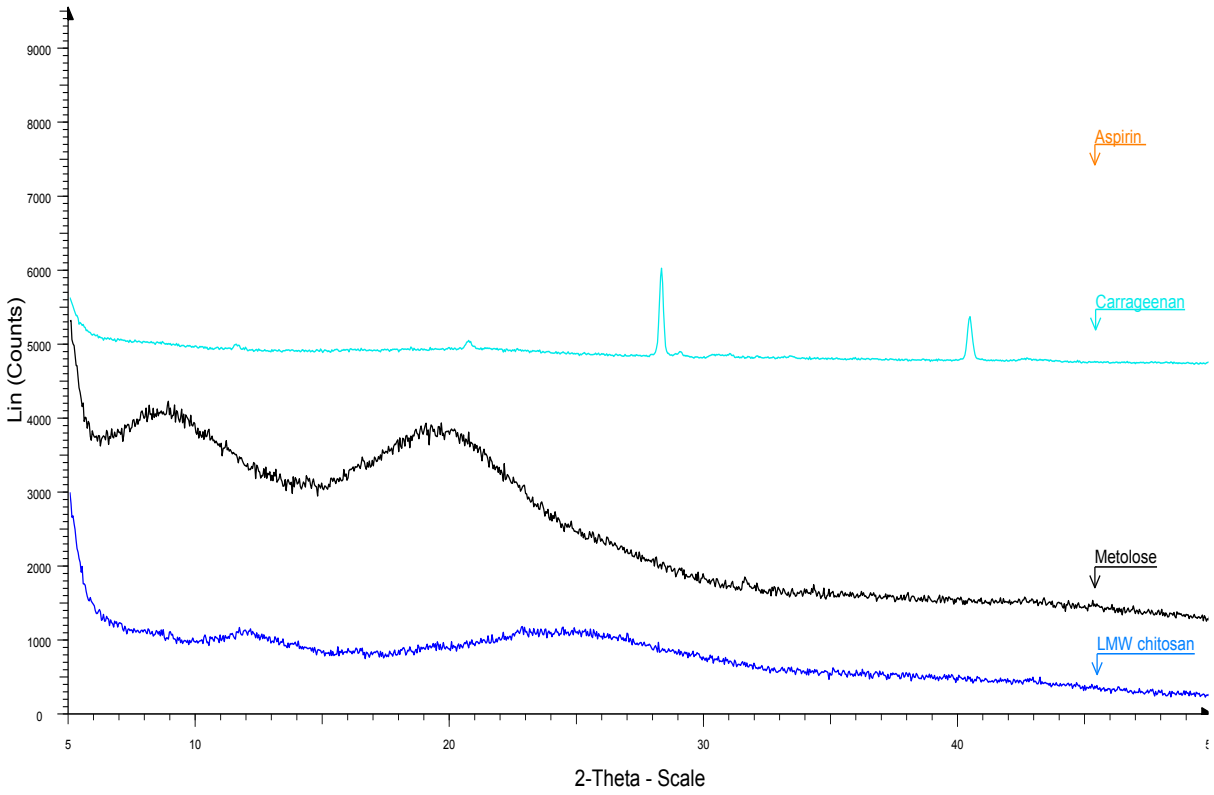

973

974 (a)

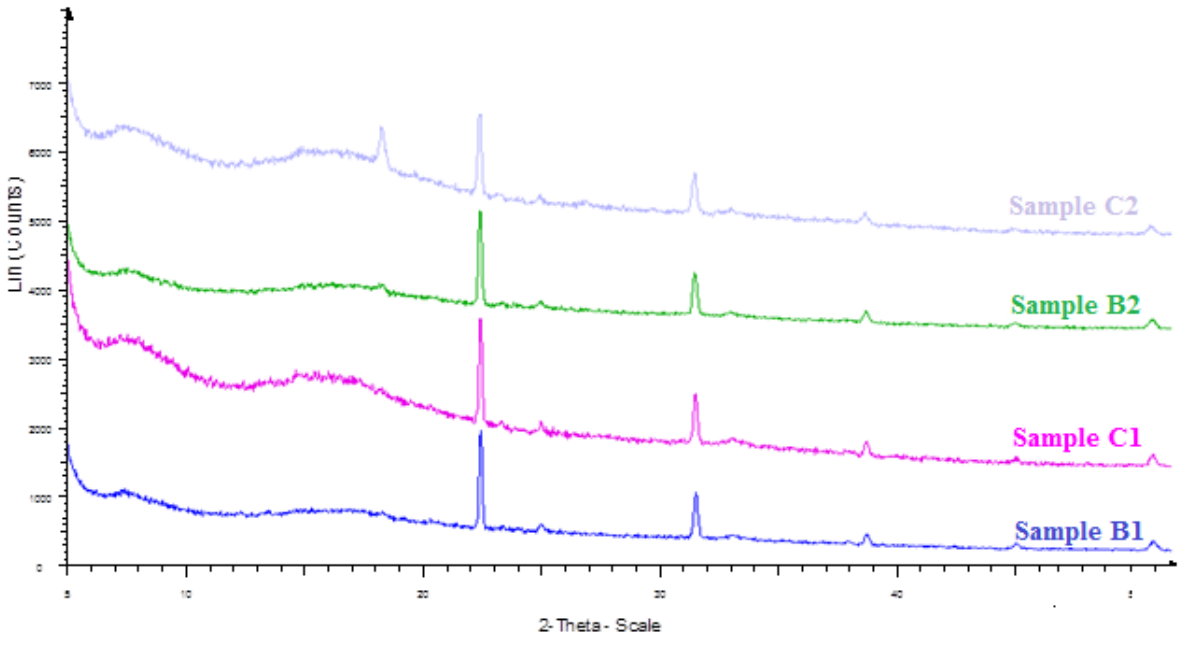

975

976 (b)

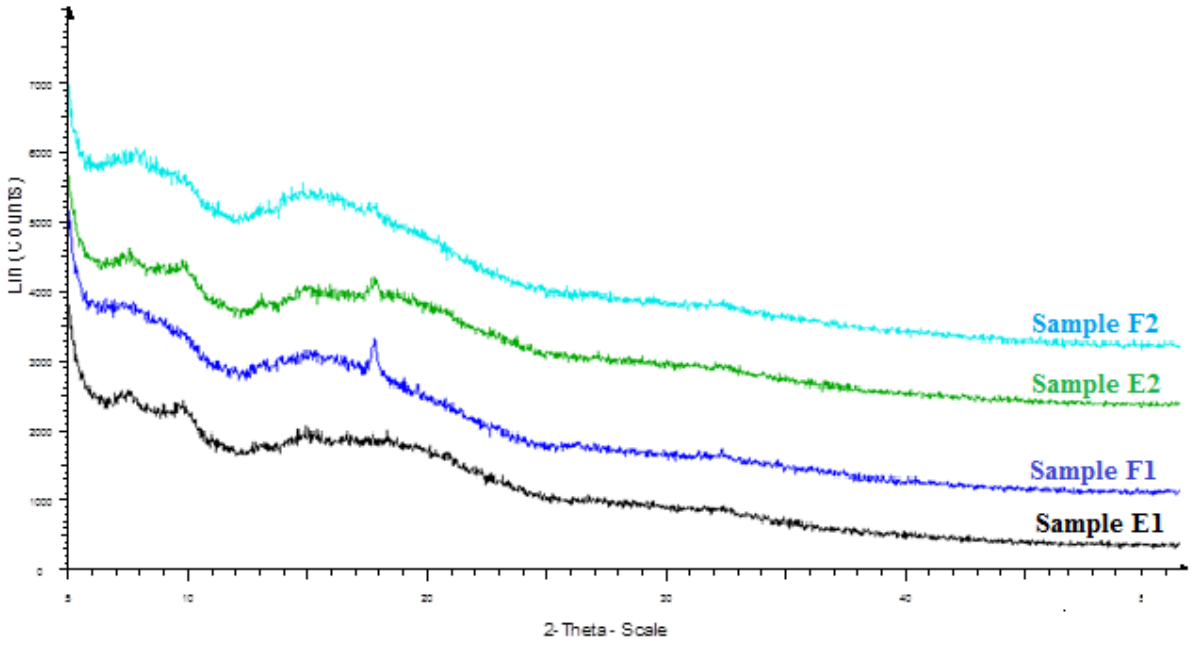

977

978 (c)

979 Figure 8. XRD-transmission diffractograms of (a) pure starting materials (b) MET:CAR
980 wafers (c) MET:CS wafers The diffractograms were obtained using a D8 Advantage X-ray
981 diffractometer. The samples were analysed in transmission mode at a diffraction angle
982 ranging from 5° to 50° 2θ, step size 0.04°, and scan speed of 0.4 s/step.

983

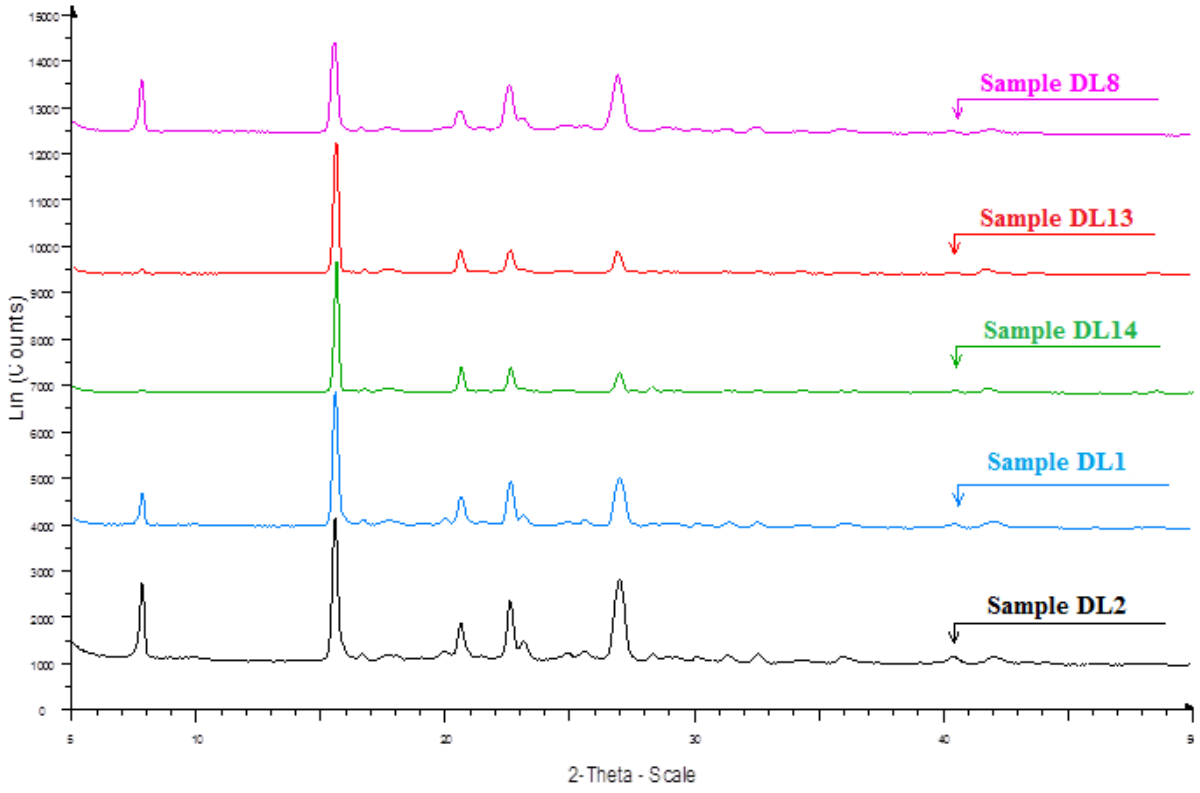

Figure 9. XRD-transmission diffractograms of DL MET:CAR, MET:CS and CAR:CS wafers. The diffractograms were obtained using a D8 Advantage X-ray diffractometer. The samples were analysed in transmission mode at a diffraction angle ranging from 5° to 50° 2θ, step size 0.04°, and scan speed of 0.4 s/step.

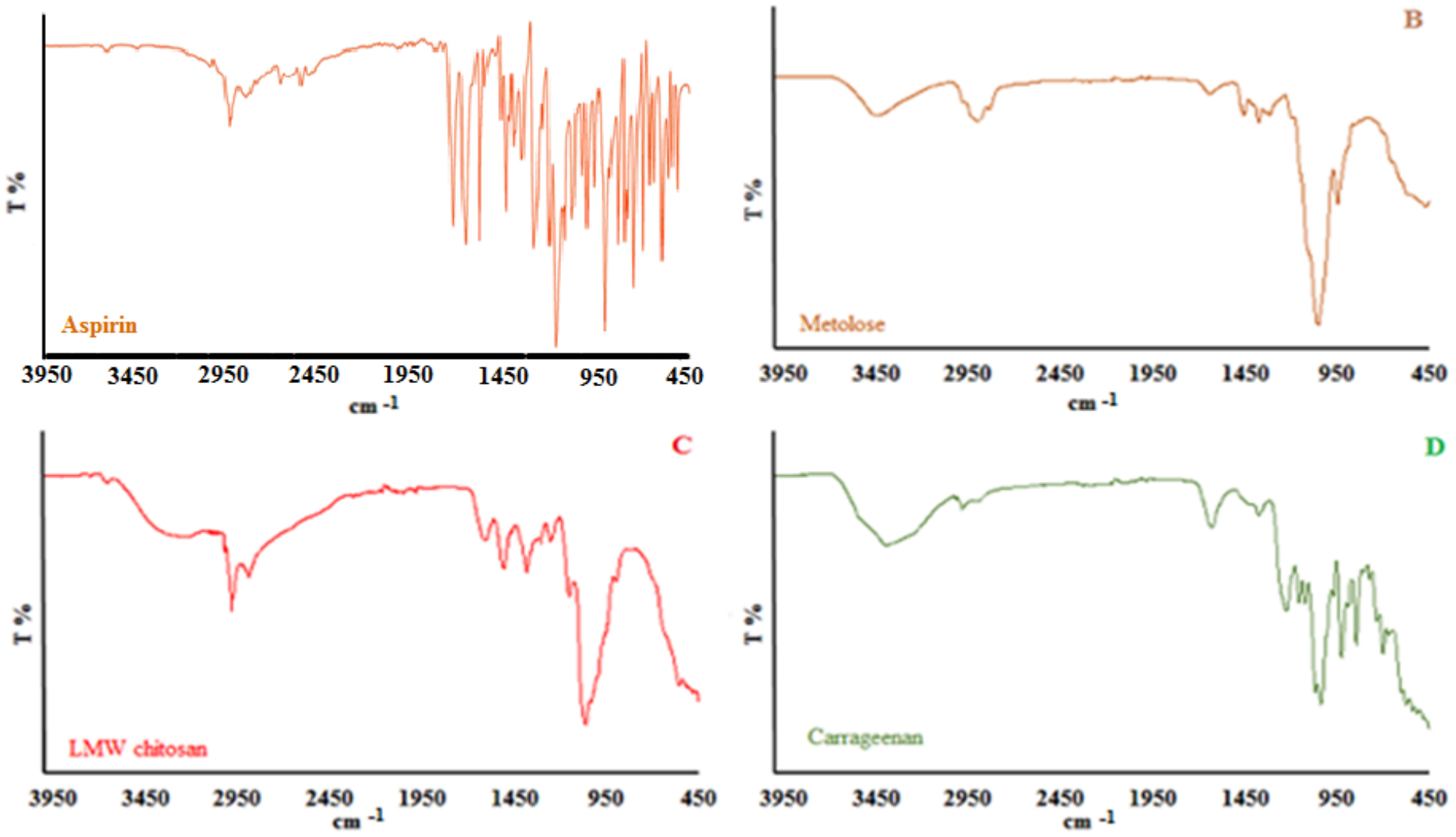
T %
Aspirin
3950 3450 2950 2450 1950 1450 950 450
cm -1
B
T %
Metolose
3950 3450 2950 2450 1950 1450 950 450
cm -1
C
T %
LMW chitosan
3950 3450 2950 2450 1950 1450 950 450
cm -1
D
T %
Carrageenan
3950 3450 2950 2450 1950 1450 950 450
cm -1

996
997 (a)

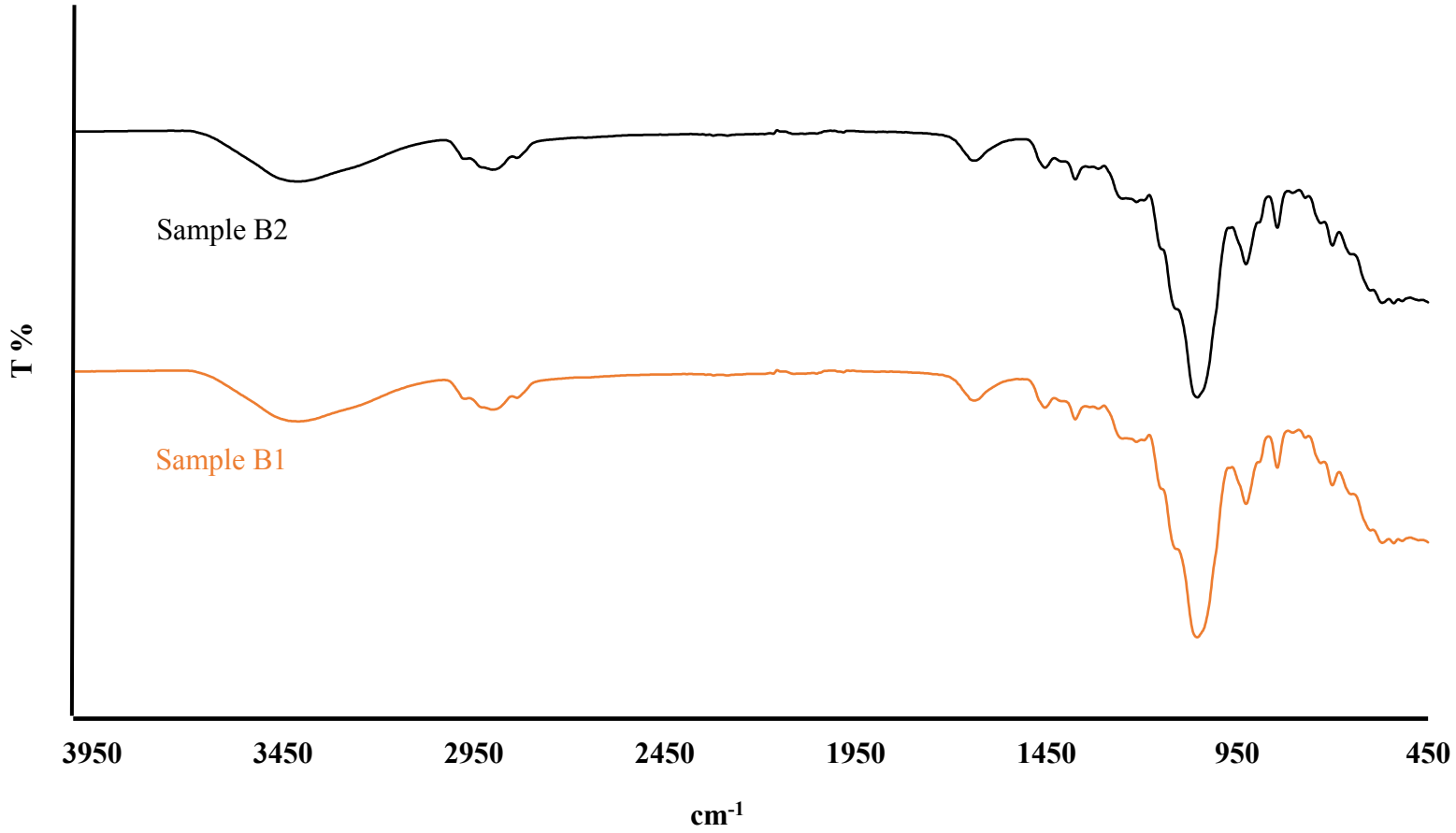
Sample B2
Sample B1
T %
3950
3450
2950
2450
1950
1450
950
450
cm-1

(b)

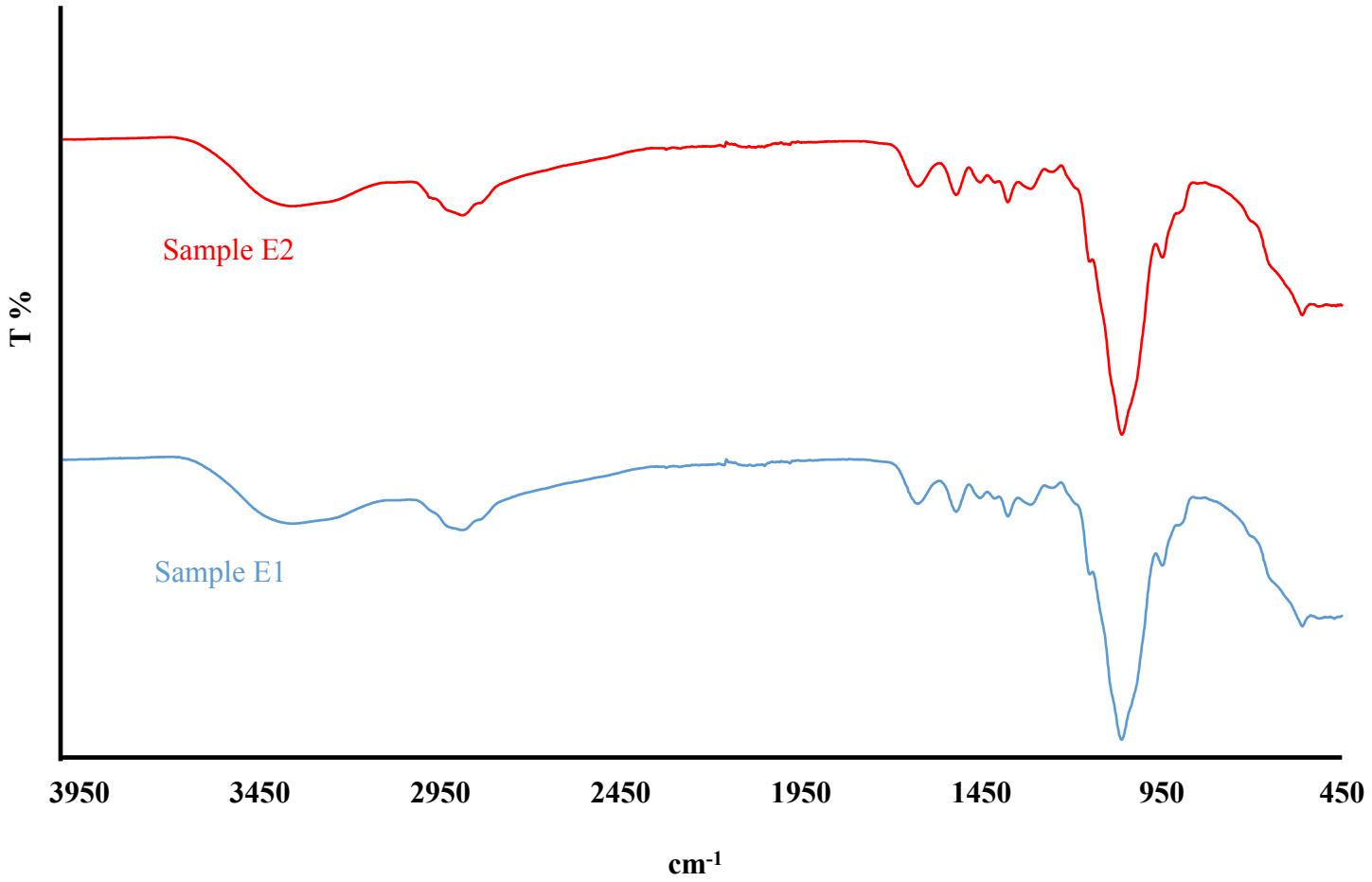

(c)

Figures 10. ATR-FTIR spectra of (a) pure starting materials and API, (b) BLK composite MET:CAR wafers, (d) composite MET:CS wafers. The spectrums were obtained from a Perkin Elmer Spectrum equipped with a diamond universal ATR unit. The resolution of the samples were recorded at 4 cm^{-1} within the range of 500-4000 cm^{-1}.

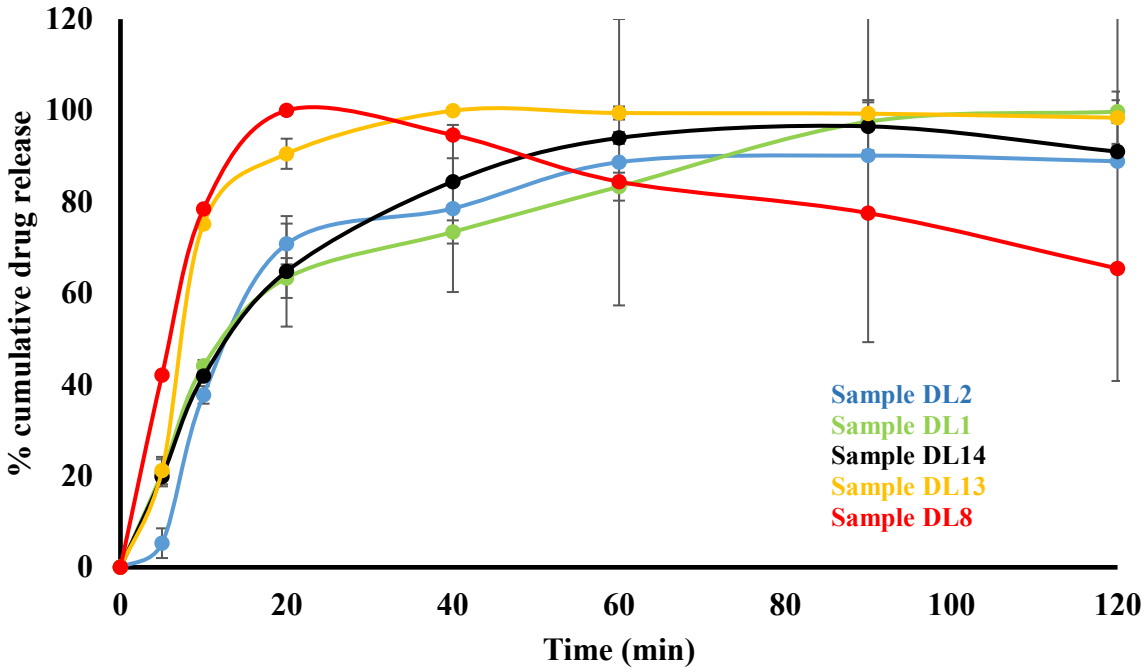

(a)

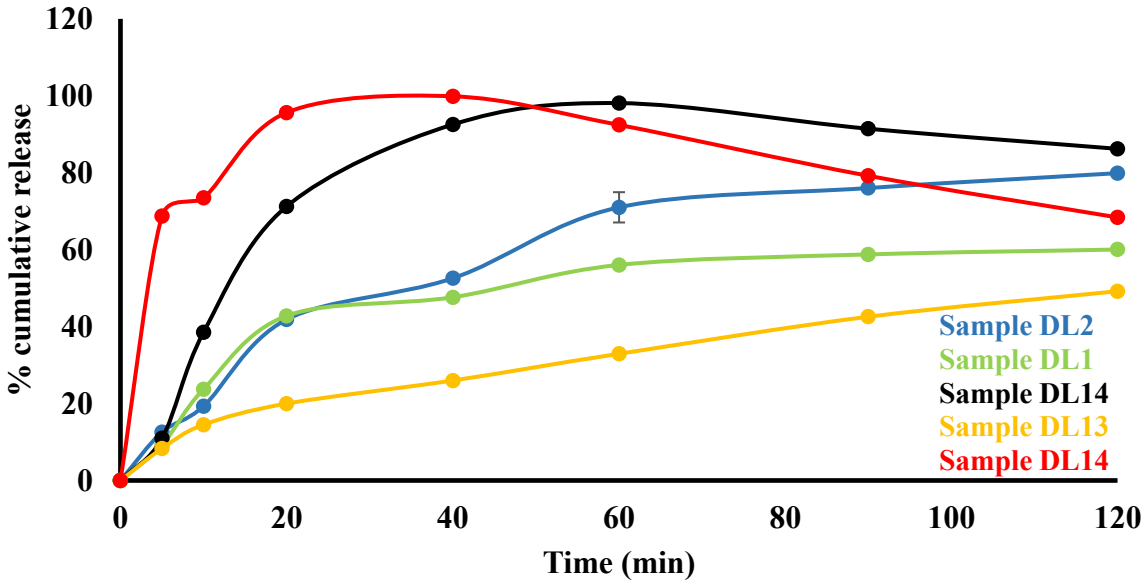

(b)

Figure 11. Drug dissolution profiles of aspirin loaded wafers prepared from ethanolic gels containing MET:CAR 1:1 and 3:1 (samples DL2 and DL1), CAR:CS 1:3 and 1:1 (samples DL13 and DL14) and MET:CS 1:3 (sample DL8) in (a) PBS at pH 6.8 ± 0.1 and (b) SS at pH 6.8 ± 0.1 (mean ± SD, n = 3).